Quaternary International
March 2019, Volume 508 Pages 70-87
https://doi.org/10.1016/j.quaint.2018.10.041
https://archimer.ifremer.fr/doc/00497/60854/

The Medieval Climate Anomaly in South America

Luening Sebastian [1,*], Galka Mariusz [2], Bamonte Florencia Paula [3], Garcia Rodriguez Felipe [4,6], Vahrenholt Fritz [5]

[1] Inst Hydrog Geoecol & Climate Sci, Hauptstr 47, CH-6315 Ageri, Switzerland.
[2] Adam Mickiewicz Univ, Fac Geog & Geol Sci, Dept Biogeog & Palaeoecol, B Krygowskiego 10, PL-61680 Poznan, Poland.
[3] Univ Nacl Mar del Plata, Lab Paleoecol & Palinol, Dept Biol, IIMYC CONICET,Fac Ciencias Exactas & Nat, Funes 3250, RA-7600 Mar Del Plata, Buenos Aires, Argentina.
[4] Ctr Univ Reg Este, CURE Rocha, Ruta 9 & Ruta 15 S-N, Rocha, Uruguay.
[5] Univ Hamburg, Dept Chem, Martin Luther King Pl 6, D-20146 Hamburg, Germany.
[6] Univ Fed Rio Grande, Programa Posgrad Oceanog Fis Quim & Geol, Inst Oceanog, Av Italia,Km 8,CxP 474, BR-96201900 Rio Grande, RS, Brazil.

* Corresponding author : Sebastian Luening, email address : luening@ifhgk.org; galka@amu.edu.pl

bamonte@mdp.edu.ar ; felipegr@fcien.edu.uy ; fritz.vahrenholt@chemie.uni-hamburg.de

Abstract :

The Medieval Climate Anomaly (MCA) is a climatic perturbation with a core period of 1000-1200 AD that is well-recognized in the Northern Hemisphere (NH). Its existence in the Southern Hemisphere (SH) and the level of synchronicity with the NH is still a matter of debate. Here we present a palaeotemperature synthesis for South America encompassing the past 1500 years based on multiproxy data from 76 published land and marine sites. The data sets have been thoroughly graphically correlated and the MCA trends palaeoclimatologically mapped. The vast majority of all South American land sites suggest a warm MCA. Andean vegetation zones moved upslope, glaciers retreated, biological productivity in high altitude lakes increased, the duration of cold season ice cover on Andean lakes shortened, and trees produced thicker annual rings. Similar MCA warming occurred in coastal seas, except in the year-round upwelling zones of Peru, northern Chile and Cabo Frio (Brazil) where upwelling processes intensified during the MCA due to changes in winds and ocean currents. MCA warming in South America and the NH appears to have occurred largely synchronous, probably reaching comparable intensities. Future studies will have to address major MCA data gaps that still exist outside the Andes in the central and eastern parts of the continent. The most likely key drivers for the medieval climate change are multicentennial Pacific and Atlantic ocean cycles, probably linked to solar forcing.

Keywords : Climate change, Late Holocene, Little Ice Age, Temperature reconstructions, Palaeoclimatology, El Nino-Southern Oscillation, Medieval Warm Period, Southern Hemisphere

Introduction

South American climate has been warming over the past 100 years, similar as most other parts of the world (Aguilar et al., 2005; Collins et al., 2009; Vincent et al., 2005). The fastest temperature rise has been recorded in Brazil, whilst the extratropical Andes and Patagonia have experienced lower warming rates (IPCC, 2007; Salvador and de Brito, 2017; Saurral et al., 2018; Soares et al., 2017; Vuille et al., 2015). Since the beginning of the 21st Century the warming trend has paused in many parts of the continent and locally even changed to cooling (Collins et al., 2009; Rosso et al., 2015; Schauwecker et al., 2014; Vuille et al., 2015). The long-term climatic warming of the past 100 years resulted in a significant retreat of Andean glaciers, whereby Venezuela already lost almost all its glaciers (Braun and Bezada, 2013; Chevallier et al., 2011; Salzmann et al., 2013; Schauwecker et al., 2014). As glaciers are continuing to shrink, it is projected that river discharge from glacierized catchments will eventually decrease, leading to water supply shortage in the tropical Andes during the dry season (Vuille et al., 2018).

Modern glacier retreat commenced after the peak of the Little Ice Age (LIA), which (besides the 8.2k event) represents the coldest phase in the global climate evolution of the past 10,000 years (Chambers et al., 2014; Marcott et al., 2013; PAGES 2k Consortium, 2013). Many Andean glaciers reached their maximum extension with their furthest down-valley positions in the mid-17th to early 18th century (Jomelli et al., 2009; Masiokas et al., 2009; Rabatel et al., 2013), corresponding to the lowest global LIA temperatures. In some parts of the Andes, such as in northern Patagonia, the most extensive glacial expansion occurred towards the end of the LIA, between the late 1700s and the 1830–1840s (Masiokas et al., 2010). The first LIA glacier advance episodes in the Andes occurred already around 1200-1350 AD (Jomelli et al., 2009; Masiokas et al., 2009), marking the transition from warm medieval conditions associated with Andean glacier retreat, to cooling and glacier advance of the LIA. The overall timing of Andean glacier evolution appears to be generally in line with the glacier history in other parts of the world which also began to advance around the 13th Century (Solomina et al., 2016).

The Andean warm phase that preceded the LIA is known as the Medieval Climate Anomaly (MCA), a recognized period of natural pre-industrial climate change associated with marked temperature and hydroclimatic variability in many parts of the world (e.g. Graham et al., 2011; Lüning et al., 2018; Lüning et al., 2017; Mann et al., 2009). The anomaly was first described by Lamb (1965) as 'Early Medieval Warm Epoch', which subsequently changed in the literature to 'Medieval Warm Period' (MWP), and later to MCA. It is generally agreed today that the core period of the MCA encompasses ca. 1000-1200 AD, even though different time schemes and durations have historically been used in the literature (e.g. Crowley and Lowery, 2000; Esper and Frank, 2009; Mann et al., 2009). The MCA represents the most recent natural warm phase and provides crucial context information for our Current Warm Period (CWP) and its warming process.

The first temperature reconstruction published for (southern) South America covering the last millennium was published by Neukom et al. (2011). In their reconstruction of summer temperatures the period 900-1350 AD showed significantly elevated values that even partly exceeded modern levels. The second half of the MCA, however, was suggested to be rather cold and the later part of the LIA rather warm. As the reconstruction only included two proxy series that reached back to the MCA (Quelccaya ice core [our site 27] and Laguna Aculeo [our site 33]), the early part of the reconstruction is only weakly supported by data and therefore awaits further refinement. In particular, mismatches with the Andean glacier history need to be clarified. Likewise, the subsequently published South America reconstruction by the PAGES 2k Consortium (2013) only included the same two proxy series. Southern Hemisphere temperature reconstructions by Mann et al. (2008) and Neukom et al. (2014) employed a few more MCA sites which at least in part, however, represent more likely hydroclimate proxies (see discussion part).

The field of palaeoclimatology has made major progress over the past 15 years during which a great number of high- and medium-resolution case studies were published, reconstructing climate change of the past millennia. In many parts of the world, regional data coverage has now reached a point which allows compiling palaeoclimate maps for well-defined time intervals. In this contribution we are attempting to integrate all available published quantitative and qualitative palaeotemperature records of the MCA in South America based on 76 land and marine study sites (Table 1). We are combining the conventionally used ice core and lake productivity data with palaeotemperature proxies from palynology (e.g. Flantua et al., 2016), tree rings, moraine age dating, marine cores as well as various other methodologies and palaeoclimatic archive types (e.g. McGregor et al., 2015; Moy et al., 2009). Detailed site descriptions and discussions can be found in the Data Supplement to this paper. South America is of particular interest as it was long unclear whether the MCA was also developed in the Southern Hemisphere, and if typical MCA warming could be found here, like already documented in some detail for the Northern Hemisphere (Diaz et al., 2011; Mann, 2002). This data review aims to help answer (1) if MCA climate change followed any regional patterns across the continent, (2) whether the MCA temperature evolution in South America was synchronous or significantly different to events on the Northern Hemisphere, and (3) which are the possible drivers of multicentennial medieval climate change in South America.

Modern Climate Elements of South America

Climate zones

According to the Köppen-Geiger climate classification (e.g. Köppen, 1918), South America can be grouped into tropical, arid and temperate climate zones. The northern half of the continent is generally tropical, whilst the southern half is dominated by subtropical, temperate/highly seasonal climate (Fig. 1). The tropical wet climatic zone is characterized by high rainfall and high temperatures throughout the year. Most of this region is covered by the Amazon rain forest, but tropical wet climate also occurs in the Guayanas, along the southeastern Brazilian coast and in southwestern Venezuela. The tropical rain forests are flanked by large areas of tropical wet and dry climate. These savannahs are associated with warm climates and seasonal rainfall. They are are located in southern Brazil, Venezuela and northern Colombia. Humid subtropical climate occurs in southern Paraguay, southern Brazil, Uruguay, and northeastern Argentina where summers are warm and humid, with rainy winters. Mediterranean climate is found in central Chile with warm, dry summers and cool, rainy winters. The Chilean Matorral vegetation consists of a shrubland plant community, composed of hard-leaved shrubs, small trees, cactus, and bromeliads. Cool, rainy winters and mild, rainy summers occur along the Patagonian coast in southern Chile and southern Argentina, representing marine west coast climate. High altitude climatic conditions prevail in the high Andes, where in some places local ice caps and ice fields exist. Temperatures are moderate to cold, depending on elevation. Semiarid conditions in northern Argentina and eastern Brazil form the basis of a Steppe climate which is associated with grass-covered plains and desert shrub vegetation. Desert climate occurs along the Pacific coast in central and northern South America, including the Atacama Desert, the driest desert of the world. The Andes act as a barrier to moisture-bearing Easterlies, whilst on the western side the cold Peru Current prevents the formation of coastal clouds. Another arid region is the Patagonian Desert in Argentina which is a large cold winter desert. Humid Westerlies originating from the Pacific transport large amounts of rain to the southern coastal portions of Chile before colliding with the Andes. The eastern side of the southern Andes lies in the rain shadow.

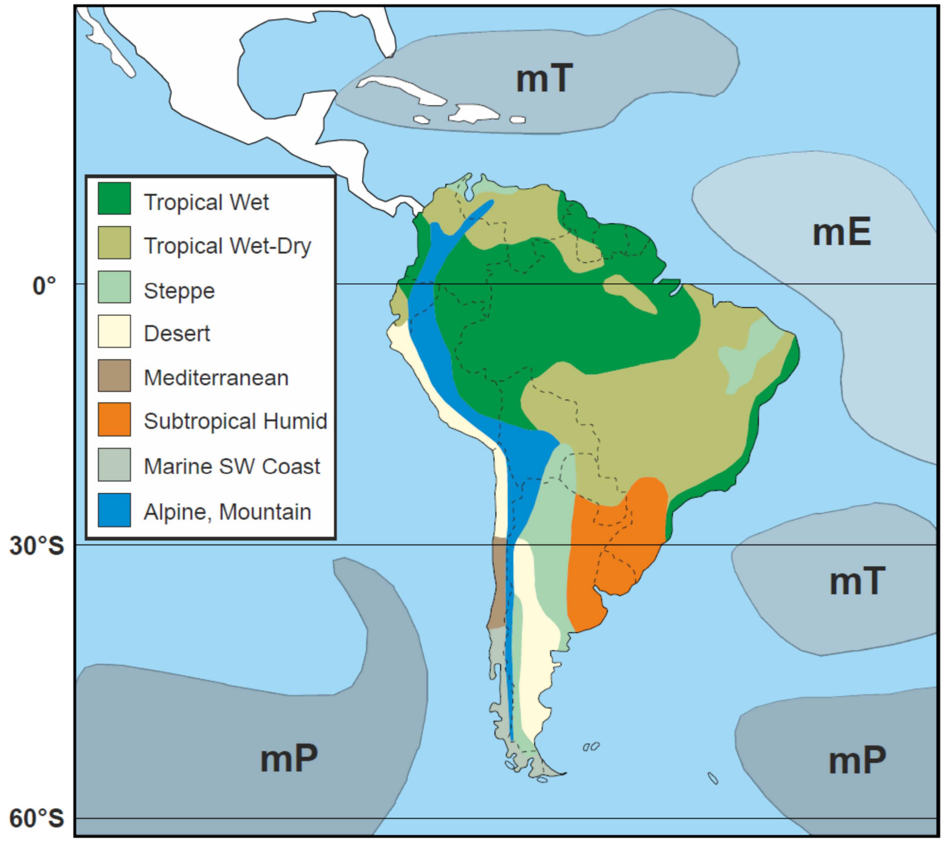

Fig. 1. *Climatic zones and air masses in South America. Air masses: mE=maritime equatorial, mT=maritime tropical, mP=maritime polar.*

Winds and air masses

The Equator crosses northern South America in the Brazilian Amazon Basin, Colombia and Ecuador (Fig. 1). The Hadley Cells on either side lead to the development of Northeast and Southeast Trade Winds in the northern and southern hemispheres, respectively. The southern limit of the Southeast Trades is formed by a belt of atmospheric high pressure around latitudes of 30°S in southern Brazil and northern Argentina, the subtropical ridge. To the south of this ridge, Westerlies dominate in southern Argentina and southern Chile, associated with the Ferrel Cell. Three types of maritime air masses surround South America.

An equatorial air mass is associated with the equatorial low pressure zone, tropical air masses occur in the Carribbean and along the Subtropical Ridge, and polar air masses of subantarctic origin affect Patagonia (Fig. 1). Rainfall in central South America is strongly dependent on the South American Summer Monsoon (SASM) which is influenced by the Intertropical Convergence Zone (ITCZ) and the South Atlantic Convergence Zone (SACZ) (Novello et al., 2017). The SASM was relatively strong during the LIA but much weaker during the MCA and Current Warm Period (Vuille et al., 2012).

Currents and Upwelling zones

Oceanography of the seas around South America is controlled by several important currents and upwelling zones which need to be taken into account in the interpretations of palaeotemperature records from marine cores. The upwelling systems comprise a relatively small portion of the world oceans, therefore, any climatic MCA trend needs to be regionally weighted accordingly.

Southern Caribbean Upwelling. The southern Caribbean Sea experiences strong wind-driven seasonal coastal upwelling along the coasts of Trinidad, Venezuela and Colombia which maintains a highly productive ecosystem (Kämpf and Chapman, 2016; Rueda-Roa and Muller-Karger, 2013). Upwelling is concentrated in two regions, namely a western area (N Colombia, NW Venezuela) and an eastern area (central Venezuelan coast). Upwelling is driven by alongshore trade winds that come from easterly directions and push the water offshore by means of northern hemisphere to-the-right Ekman transport. Beginning in June or July, when the ITCZ migrates north to a position near the Venezuelan coast, the trade winds diminish, and upwelling over the basin weakens or is shut off (Black et al., 2004).

Peru Upwelling. The Peru coastal upwelling occurs year-round and forms part of the global Eastern Boundary Upwelling Systems (EBUS) that are located on the eastern margins of the

Pacific and Atlantic (Tarazona and Arntz, 2001). Upwelling is caused by tradewinds blowing from southeast to northwest which push the coastal waters offshore by way of southern hemisphere to-the-left Ekman transport. The warm, usually nutrient-depleted surface water is replaced by cooler, nutrient-rich water that rises from the deep. The upwelling zone lies at the northern end of the Humboldt (Peru) Current which brings cold Antarctic water to the region and takes a westward turn off Peru towards the open Pacific. During the last 50 years, Peru upwelling has been intensifying (Narayan et al., 2010).

Galapagos Upwelling and Current Systems. Waters of the archipelago show a wide range of temperature and salinity due to the interaction of several different current systems. The western part of the Galapagos Islands experiences upwelling. Here, the eastward-flowing Pacific Equatorial Undercurrent (Cromwell Curent), a subsurface current, collides with the western Galapagos seamounts at a water depth of 50 m (Liu et al., 2014; Martínez-Ortiz et al., 2015). As a result relatively colder, nutrient-rich water is forced to the surface, causing major upwelling associated with the highest biological production in the archipelago. The eastern side of the islands receive cool upwelled water from the Peru Upwelling System through the westward-flowing South Equatorial Current. The far northern Galapagos region is characterized by warmer, fresher water with the greatest mixed layer depth as a result of Panama Current waters entering from the northeast (Liu et al., 2014).

Chile Upwelling. Coastal upwelling along the Chilean coast forms the basis for one of the world's biologically most productive ocean regions. Along the coast of northern and central Chile, upwelling is localised and its occurrence changes from being mostly continuous (aseasonal) in northern Chile to a more seasonal pattern in central and southern Chile, including Patagonia (Escribano and Schneider, 2007; Letelier et al., 2009; Oyarzún and Brierley, 2018; Thiel et al., 2007). In the seasonal upwelling regions, upwelling-favorable winds predominate during austral spring and summer, concurring with the southernmost position of the subtropical anticyclone in the East South Pacific. Downwelling occurs in winter. Large-scale climatic phenomena (El Niño Southern Oscillation, ENSO) are superimposed onto this regional pattern, which results in a high spatiotemporal heterogeneity.

Brazil Upwelling. Coastal upwelling occurs on the Brazilian shelf in three different regions, namely off southern Bahia, off Cabo Frio and off Cabo de Santa Marta (Kämpf and Chapman, 2016). These seasonal upwelling systems represent an anomaly in that they are located on the western side of the Atlantic Ocean. Northeasterly winds run parallel to the coastline and push surface water offshore by way of to-the-left southern hemisphere Ekman transport (Mahiques et al., 2005; Valentin, 2001). The water is replaced by upwelling of deep, cold South Atlantic central water (Palóczy et al., 2014). Cabo Frio upwelling is most intense in the spring and summer season (Coelho-Souza et al., 2012).

Brazil Current / Malvinas Current interaction zone. The Brazil Current is the Western Boundary Current of the South Atlantic Ocean and flows southwards along the Brazilian coast. The current carries warm and salty waters poleward. At a position off Uruguay the Brazil Current collides with a northward branch of the Antarctic Circumpolar Current, the Malvinas (Falkland) Current, which transports cold and relatively fresh subAntarctic waters equatorward (Piola and Matano, 2017). The collision between these distinct water masses, together with the freshwater discharge from Río de la Plata, generates one of the most energetic regions of the world ocean: the Brazil/Malvinas Confluence (BMC). The collision of the Brazil and Malvinas currents spawns one of the most spectacular eddy fields of the global ocean (Piola and Matano, 2017). The Brazil Current underwent major changes during the transition from the latest Pleistocene to the Holocene (Gu et al., 2018).

Fig. 2. *Location map of studied sites. Key to site numbers in Table 1. Red lines mark correlation panels illustrated in Supplement (with respective figure number). For zoom location maps see Supplement Figs. S1, S3, S6, S9, S11, S18.*

Material and Methods

Literature review

The mapping project is based on an intense iterative literature screening process during which a large number of published South American palaeotemperature case studies were evaluated towards their temporal coverage, type of climate information and data resolution. Suitable papers including the MCA core period 1000-1200 AD were selected for a thorough analysis. A total of 76 South American localities with one or more MCA palaeotemperature proxy curves or related data were identified (Fig. 2, Tables 1 and S1).

Palaeoclimate archives and data types

MCA climate reconstructions of the high-graded publications comprised of several natural and historical archives, namely (1) sediment cores from offshore marine, lakes, peatlands, (2) ice cores from Andean ice caps, (3) age dating of glacier moraines, (4) tree rings, and (5) historical accounts. Data types include (a) palaeontology: pollen assemblages tracking vertical shifts in tree line and Andean vegetational belts, opal phytoliths, chironomid-inferred lake temperatures, diatom assemblages as proxies for ice cover and precipitation, tree rings, planktic foraminifera assemblages in marine cores; (b) inorganic geochemistry: Mg/Ca planktonic foraminifera sea surface temperature (SST), $\delta^{18}O$ and δD in ice cores, NH_4-based temperatures of ice cores, $\delta^{18}O$ in foraminifera, $\delta^{18}O$ of *Mytilus edulis* shells, $\delta^{13}C$-based stalagmite temperatures, chlorine as sea water proxy; (c) organic geochemistry: total organic carbon, hydrogen index, Uk'37 SST, brGDGT lake temperatures, pigment-based lake temperatures, bSi-based temperatures; (d) geophysics: magnetic susceptibility, radiocarbon ^{14}C and ^{10}Be age dating of glacier moraines; (e) sedimentology: Fe, K, Ca, Sr, Zr, Ti as glacier activity proxy of clastic sediments in proglacial lakes, clay-based temperatures, deposition time as ice cover duration proxy, varve-based temperatures, sortable silt.

Data processing and visualisation

Qualitative. Key information of the identified publications were captured on a georeferenced online map which is freely available to all interested members of the palaeoclimate science community for research and reference purposes (http://t1p.de/mwp). The MCA palaeotemperature was visually assessed and compared to the phases preceding and following the anomaly. The MCA conditions were colour-coded with red dots marking a trend towards warmer conditions while blue dots represent cooling. The colour-coding provides much-needed initial orientation in the complex global MCA climate puzzle.

Quantitative. In order to robustly document, visualise and analyse MCA palaeoclimatic variability, all relevant climate curve data were collected in digital form for flexible plotting and curve correlation. The tabulated data were retrieved (a) from palaeoclimate online data repositories (mainly Pangaea, NOAA's National Climatic Data Center NCDC, and data supplements of papers), (b) from authors by email request and (c) by digitizing and vectorising using WebPlotDigitizer (https://automeris.io/WebPlotDigitizer/). Data sources for each site are listed in Table S1. All curve data have been loaded into Lloyd's Register's software IC™ which serves as a common database and correlation tool in the MCA mapping project. IC™ was originally developed for geological well correlations in the areas of water, minerals and petroleum exploration. The software reliably handles large amounts of fully customizable curve data types related to georeferenced wells. By way of technology transfer we are introducing well correlation software to the field of the climate sciences which allows fast and flexible comparison of climate curves. Another advantage is the advanced visualisation and shading of peak and trough curve anomalies, a functionality which lacks in most standard spreadsheet software packages. See Lüning et al. (2017) for details on the workflow. The vectorized South America base map in this paper was sourced from http://www.d-maps.com.

Challenges

Like any other regional palaeoclimatic synthesis, the current South America palaeotemperature MCA mapping effort is subject to a number of challenges. Palaeoclimatology is not an exact mathematical science, nevertheless provides crucial proxy data for the palaeoclimatological context and model calibration. A probabilistic approach is needed whereby the most likely scenario is selected from the set of available proxies. Issues identified in the current synthesis include (1) low resolution palaeoclimate data, (2) limited age control, (3) conflicting information from multiple proxies. See Lüning et al. (2017) for a more detailed discussion.

Results

A total of 76 study sites have been identified in South America which are mostly concentrated along the Andes, but with patchy data also from other areas (Fig. 2, Table 1). Detailed site descriptions and palaeotemperature correlation panels are shown in the Supporting Information to this paper (texts S1-S6, figures S1-S20, Table S1). A correlation panel with 6 representative sites and the southern South American summer temperature composite by Neukom et al. (2011) from the study area is illustrated in Figure 3. Proxy plots start at 500 AD in order to also document the climate trends preceding the MCA and place the anomaly in a multi-centennial context.

No.	Locality	Region	Country	Archive	Proxies	Studies
1	CAR7-2 and MC-4	Cariaco Basin	Venezuela	Marine core	Uk’37 SST, $\delta^{18}O$ of *Globigerina bulloides*	Goni et al. (2004), Black et al. (2004)
2	PL07-39PC	Cariaco Basin	Venezuela	Marine core	Mg/Ca SST	Lea et al. (2003)
3	Laguna de Mucubaji	Cordillera de Mérida, Andes	Venezuela	Lake core	Fe	Stansell et al. (2005), Stansell et al. (2014)

4	Paramo de Piedras Blancas	Cordillera de Mérida, Andes	Venezuela	Peat core	Pollen as treeline proxy	Rull et al. (1987)
5	Laguna de Los Anteojos	Cordillera de Mérida, Andes	Venezuela	Lake core	Fe	Stansell et al. (2014)
6	Laguna de Montos	Cordillera de Mérida, Andes	Venezuela	Lake core	Magnetic susceptibility	Stansell et al. (2014)
7	Llano Grande peatbog	Páramo de Frontino	Colombia	Peat core	Pollen as treeline proxy	Muñoz et al. (2017), Velásquez-Ruiz and Hooghiemstra (2013)
8	El Triunfo wetland	Central Cordillera	Colombia	Peat core	Pollen as treeline proxy	Giraldo-Giraldo et al. (2018)
9	Laguna Chingaza	Eastern Cordillera	Colombia	Lake core	brGDGT temperatures	Bixler (2012)
10	Laguna La Cocha	Eastern Cordillera	Colombia	Lake core	Pollen as treeline proxy	González-Carranza et al. (2012)
11	Guandera peat bog	Eastern Cordillera	Ecuador	Peat core	Pollen as treeline proxy	Moscol Olivera and Hooghiemstra (2010)
12	Lagunas de Mojanda complex	northern Ecuadorian Andes	Ecuador	Lake marsh core	Pollen as treeline proxy	Villota et al. (2017)
13	Laguna Pindo	Ecuadorian Andes	Ecuador	Lake core	Chironomid temperatures	Matthews-Bird et al. (2016)
14	Tres Lagunas	Western Cordillera	Ecuador	Peat core	Isoetes	Jantz and Behling (2012)
15	M772-056	Gulf of Guayaquil	Peru	Marine core	Uk'37 SST	Seillès et al. (2016)
16	M772-059	Gulf of Guayaquil	Peru	Marine core	Uk'37 SST, SubSST Mg/Ca derived from N. dutertrei	Nürnberg et al. (2015)
17	El Junco Lake	Galápagos Islands	Ecuador	Lake core	Tychoplankto-nic to epiphytic diatom ratio	Conroy et al. (2008), Conroy et al. (2009)
18	KNR195-5 MC42C	Galápagos Islands	Ecuador	Marine core	Mg/Ca SST	Rustic et al. (2015)
19	Huascarán ice core	Cordillera Blanca	Peru	Ice core	$\delta^{18}O$	Thompson et al. (1995), Thompson (1995)
20	Laguna	Cordillera	Peru	Lake core	Ca, Sr, Zr, ms	Stansell et al. (2013)

	Queshquecocha	Blanca				
21	Laguna Jahuacocha	Cordillera Huayhuash	Peru	Lake core	K, Ca, Ti, ms	Stansell et al. (2013)
22	Laguna Lutacocha	Cordillera Raura	Peru	Lake core	Ca, Ti, Fe, ms	Stansell et al. (2013)
23	G10	central Peruvian continental shelf	Peru	Marine core	TOC, HI	Salvatteci et al. (2016)
24	Marcacocha lake basin	Cusco region	Peru	Lake core	Pollen	Chepstow-Lusty et al. (2009), Sterken et al. (2006)
25	Tarn Challpacocha	Southern Peruvian Andes	Peru	Lake core	Total Organic Matter	Stroup et al. (2015)
26	Qori Kalis outlet glacier	Southern Peruvian Andes	Peru	Moraine ages	^{10}Be moraine chronology	Stroup et al. (2014)
27	Quelccaya ice cap	Southern Peruvian Andes	Peru	Ice core	$\delta^{18}O$	Thompson et al. (2013), Thompson et al. (1986), Bird et al. (2011b)
28	Tarn Yanacocha	Southern Peruvian Andes	Peru	Lake core	Total Organic Matter	Stroup et al. (2015)
29	Nevado Illimani ice core	Cordillera Real	Bolivia	Ice core	NH_4-based temperatures, δD	Kellerhals et al. (2010), Ramirez et al. (2003)
30	Nevado Sajama ice core	Bolivian Andes	Bolivia	Ice core	$\delta^{18}O$, 3 decade running mean	Thompson et al. (2003)
31	Inglesa Bay	Atacama region	Chile	Marine core	Uk'37 SST	Castillo et al. (2017)
32	Laguna Chepical	high central Andes of Chile	Chile	Lake core	Clay-based temperatures, diatom-based ice cover length	de Jong et al. (2013), Martel-Cea et al. (2016)
33	Laguna Aculeo	Coastal Cordillera	Chile	Lake core	Pigment-based temperatures	von Gunten et al. (2009)
34	Laguna San Pedro	Chilean Andes	Chile	Lake core	Deposition time	Fletcher and Moreno

						(2012)
35	Captren	Chilean Andes	Chile	Tree rings	Tree rings	Aguilera-Betti et al. (2017)
36	Rio Alerce	Northern Patagonia	Argentina	Tree rings	Tree Rings	Villalba (1994), Villalba et al. (1990)
37	Costa del Osorno	Coastal central Chile	Chile	Tree rings	Tree Rings	Rigozo et al. (2008a)
38	GeoB 3313-1 and ODP 1233	offshore central Chile	Chile	Marine core	Uk'37 SST	Lamy et al. (2002), Euler and Ninnemann (2010)
39	Abtao	Coastal central Chile	Chile	Tree rings	Tree Rings	Jalabert (2002)
40	GeoB 7186-3	Offshore Chile	Chile	Marine core	Uk'37 SST	Mohtadi et al. (2007)
41	CF7-PC33	Jacaf Channel	Chile	Marine core	Uk'37 SST	Sepúlveda et al. (2009)
42	Laguna Escondida	Northern Patagonia	Chile	Lake core	bSi-based temperatures	Elbert et al. (2013b)
43	MD07-3088	Aysen fjords	Chile	Marine core	$\delta^{18}O$ *G. bulloides*	Siani et al. (2013)
44	Soler Glacier	Northern Patagonian Icefield	Chile	Glacier dating	radiocarbon ages of In situ tree remains	Glasser et al. (2002)
45	Lago Plomo	Northern Patagonian Icefield	Chile	Lake core	Varve-based temperatures	Elbert et al. (2013a)
46	Glaciar Jorge Montt	Southern Patagonian Icefield	Chile	Glacier dating	radiocarbon ages of recently exposed trees	Rivera et al. (2012)
47	Lago del Desierto	Southern Patagonian Icefield	Argentina	Lake core	Ca/Ti, ms	Kastner et al. (2010)
48	Herminita Peninsula	Southern Patagonian Icefield	Argentina	Moraine dating	Moraine age dates	Kaplan et al. (2016), Strelin et al. (2014)
49	Patagonian Icefield	Southern Patagonian Icefield	Chile	Moraine dating	age dating of glacial elements	Aniya (2013)
50	JPC-42	Europa and Penguin fjords	Chile	Marine core	Uk'37 SST	Caniupán et al. (2014)
51	MD07-3124	Canal	Chile	Marine core	Uk'37 SST	Caniupán et al. (2014)

		Concepción				
52	Laguna Las Vizcachas	Southern Patagonia	Argentina	Lake core	Planktic-nonplanktic diatoms, BiSi	Fey et al. (2009)
53	Tyndall Glacier	Southern Patagonia	Chile	Moraine dating	radiocarbon ages of wood, roots and other organic material	Aniya (1995)
54	CHURR	Churruca fjord	Chile	Marine core	Uk’37 SST	Caniupán et al. (2014)
55	Marcelo Arevalo cave	southernmost Chilean Andes	Chile	Cave stalagmite	δ^{13}C-based stalagmite temperatures	Mühlinghaus et al. (2008)
56	Glaciar Lengua	Gran Campo Nevado complex	Chile	Moraine dating	Dendro moraine age dates	Koch and Kilian (2005)
57	Seno Skyring Glacier lobe	southernmost Andes	Chile	Moraine dating	Moraine age dates	Kilian et al. (2007)
58	Seno Otway Fjord	Seno Otway Fjord	Chile	Marine core	Chlorine	Kilian et al. (2013)
59	MD07-3132	Strait of Magellan	Chile	Marine core	Uk’37 SST	Aracena et al. (2015)
60	Ema Glacier	Tierra del Fuego	Chile	Moraine dating	Moraine age dates	Strelin et al. (2008)
61	JPC67	Almirantazgo fjord	Chile	Marine core	Uk’37 SST	Bertrand et al. (2017)
62	Beagle Channel	Tierra del Fuego	Argentina	Marine core	δ^{18}O of *Mytilus edulis* shells	Obelic et al. (1998)
63	Isla de los Estados	Tierra del Fuego	Argentina	Peat core	*Nothofagus* pollen	Ponce et al. (2017; 2011)
64	Potiguar Basin	Equatorial Margin	Brazil	Marine core	planktic foram. SST modern analogue technique	Santos et al. (2013)
65	Pau de Fruta Peatland	Minas Gerais	Brazil	Peat core	peatland plant species composition	Schellekens et al. (2014)
66	BCCF06-03	Cabo Frio	Brazil	Marine core	Planktic foraminifera	Souto et al. (2011)

67	CF10-01B	Cabo Frio	Brazil	Marine core	Planktic foraminifera	Lessa et al. (2016; 2014)
68	LaPAS-KF02	Santos Basin	Brazil	Marine core	SST based on planktic foram. assemblages	Pivel et al. (2013)
69	GeoB6211	Pelotas Basin	Brazil	Marine core	Mg/Ca SST based on planktic foram.	Chiessi et al. (2014)
70	Pena Lagoon	Coastal Uruguay	Uruguay	Lake core	opal phytoliths	del Puerto et al. (2013)
71	Laguna Blanca	Coastal Uruguay	Uruguay	Lake core	opal phytoliths	del Puerto et al. (2006)
72	South American Plains	Border triple point	Argentina, Uruguay, Brazil	Landscape age dating	Landscape age dating	Iriondo (1999)
73	Pampean Plain	Central northern Argentina	Argentina	Landscape & history	Landscape age dating & history	Cioccale (1999)
74	Laguna Nassau	Western Pampas	Argentina	Lake core	*Celtis* pollen	Vilanova et al. (2015)
75	Lake Lonkoy	Southeastern Pampas	Argentina	Lake core	Chara oospores	Stutz et al. (2012)
76	GeoB13862-1	Mar del Plata Canyon	Argentina	Marine core	Sortable silt %, $\delta^{18}O$ *G. inflata*	Voigt et al. (2016; 2015)

Table 1. *MCA study sites in South America. For site coordinates, information on age control points and source of tabulated data see Table S1 in Supplement.*

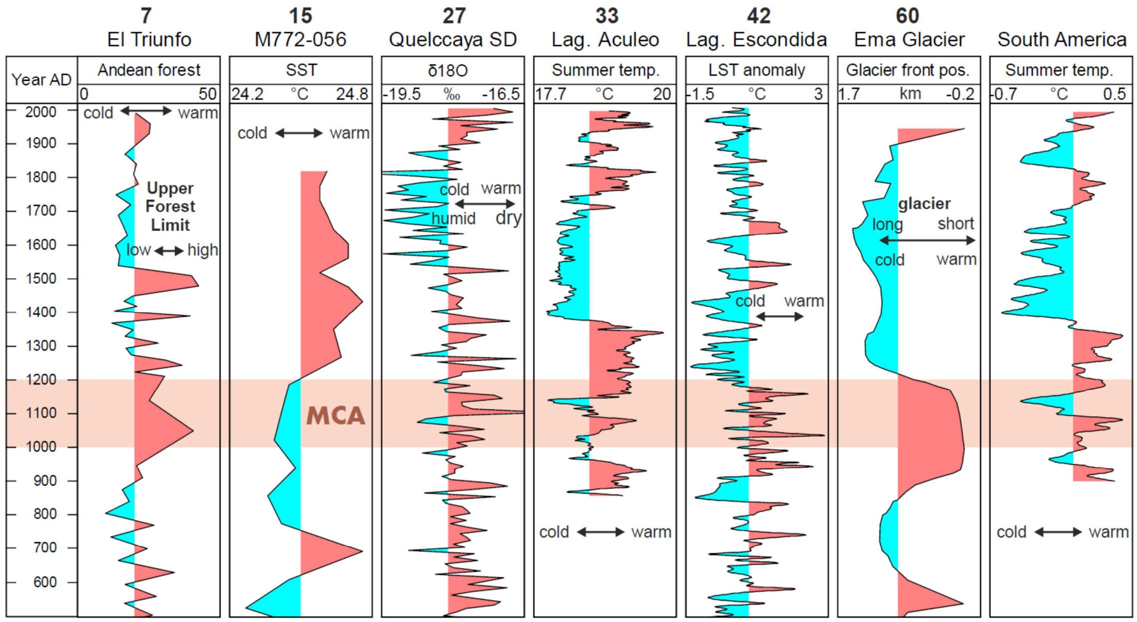

__Fig. 3.__ Temperature development in South America during the past 1500 years based on palaeoclimate proxies of selected study sites (site number stated on top). 8: El Triunfo (Giraldo-Giraldo et al., 2018); 15: M772-056 (Seillès et al., 2016); 27: Quelccaya ice cap, Summit Dome (SD) (Thompson et al., 2013); 33: Laguna Aculeo (von Gunten et al., 2009); 42: Laguna Escondida, LST=lake surface temperature (Elbert et al., 2013b); 60: Ema Glacier (Strelin et al., 2008); southern South America, 30 year LOESS filter (Neukom et al., 2011). Location map in Fig. 2.

Discussion

The North

<u>Cariaco Basin, off Venezuela</u>

A warm MCA has been documented in two marine cores from this basin, namely CAR7-2 based on Uk'37 SST (site 1, Goni et al., 2004) and the lower data resolution PL07-39PC based on Mg/Ca planktonic foraminiferal SST (site 2, Lea et al., 2003) (Fig. S2). The two cores are located in the eastern area of the Southern Caribbean Upwelling System which experiences seasonal upwelling that typically ceases in northern hemisphere summer (Rueda-Roa and Muller-Karger, 2013). Goni et al. (2004) originally interpreted the warming as a sign of reduced local upwelling during the MCA due to weakened easterly trade winds. This might have resulted from a multi-century northward shift of the ITCZ, as already suggested by previous studies (Apaéstegui et al., 2014; Bird et al., 2011b; Haug et al., 2003; Haug et al., 2001; Novello et al., 2012; Novello et al., 2018; Novello et al., 2016; Trouet et al., 2012; Vuille et al., 2012). This MCA warming effect might have been similar to the modern seasonal pattern. When the ITCZ migrates northwards during the boreal summer, trade winds over the basin weaken and upwelling is interrupted, resulting in SST warming (Peterson and Haug, 2006).

Surprisingly, however, the Cariaco SST development of the past 1500 years matches quite well with temperature trends observed in many other northern Andean land studies (sites 3-8, 11-13). The general pattern comprises of a warm MCA, followed by major LIA cooling and a fast modern temperature rebound. Lea et al. (2003) had already noted the great synchronicity of the Cariaco SST with the international reference site of the Greenland GISP2 ice core temperature record for the past 25,000 years. The SST changes in the Cariaco Basin are therefore unlikely to represent a response to upwelling alone. Black et al. (2007) suggested that the Carioca Basin palaeotemperature changes are not necessarily related to local upwelling variability but instead represent rather wider regional conditions in the Caribbean and western tropical Atlantic. A comparison of the Mg/Ca SST record to *Globigerina bulloides* abundance - a proxy for upwelling and trade wind variability in the Cariaco Basin - reveals a very low similarity between the two records (Black et al., 2007; Black et al., 1999; Lea et al., 2003). The reconstructed SST signal may be dominated by the non-upwelling season which could explain the mismatch between SST and upwelling proxies (Goni et al., 2004). Likewise, temperature differences observed in the Uk’37 and Mg/Ca SST reconstructions before and after the MCA may be due to similar seasonal proxy bias and/or poor data resolution of site 2.

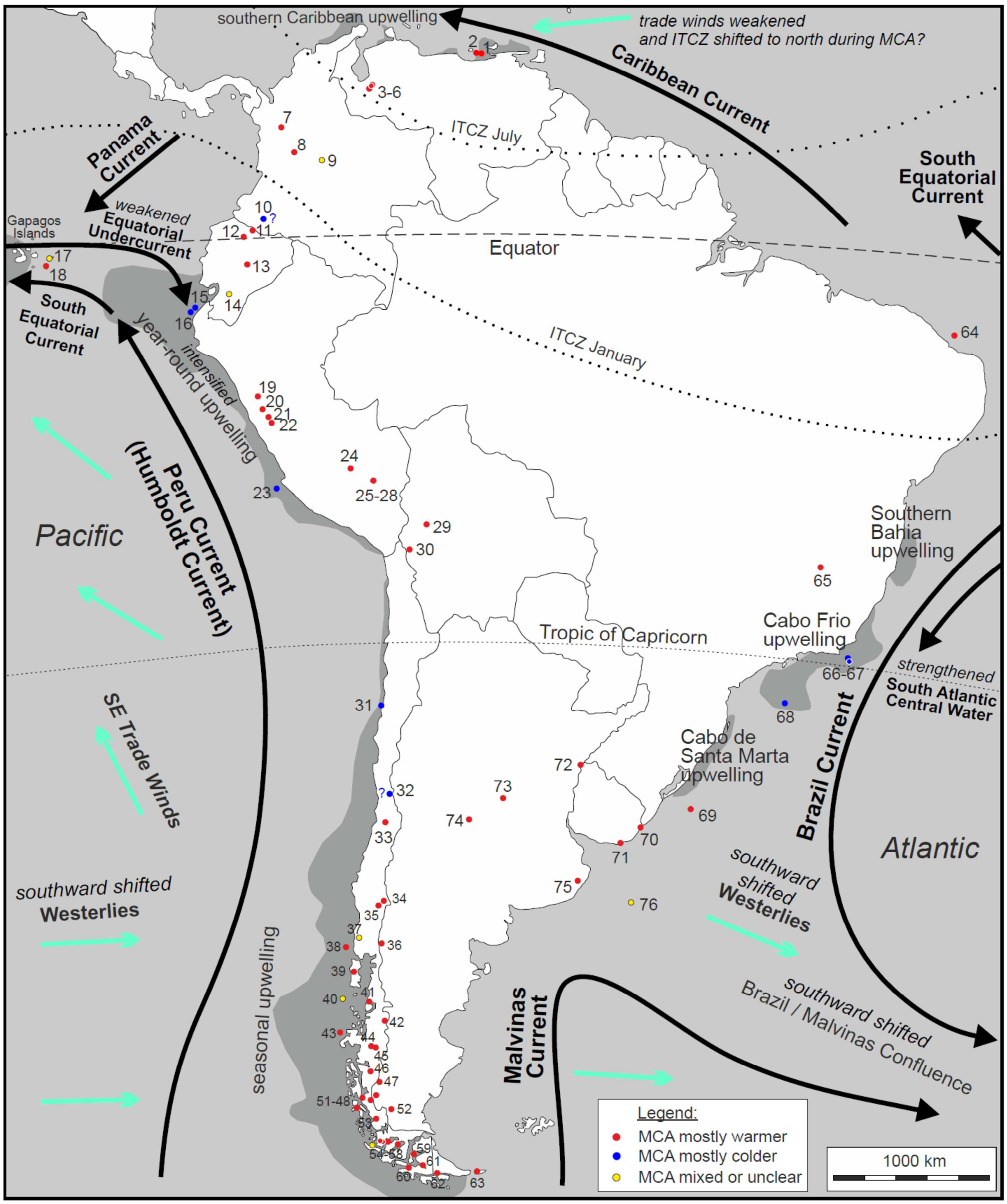

__Fig. 4.__ Palaeotemperature trends during the MCA with color-coded study sites showing changes to warmer (red) and colder (blue) climate. Yellow dots mark locations with mixed MCA climate signals, conflicting proxies, low data resolution or lack of information. Numbers

refer to study sites as shown in Table 1. Dark grey regions mark present-day upwelling systems as mapped by elevated concentration of ocean chlorophyll (Capone and Hutchins, 2013). Winds are illustrated by green (after Lechleitner et al., 2017) and ocean currents by black arrows. For zoom location maps see Supplement Figs. S1, S3, S6, S9, S11, S18.

<u>*Northern Andes*</u>

The vast majority of studies in the northern Andes show a warm MCA. Stansell et al. (2014) studied three lakes in the Andean Cordillera de Mérida in NW Venezuela at heights ranging from 3500 to 4100 m asl. that are well situated to record changes in glacial activity in the respective updip valleys and catchment areas (sites 3, 5, 6; Figs. S1 and S2). Clastic sediment influx decreased during the MCA which is thought to reflect reduced glacier erosion during an ice margin retreat phase. According to Stansell et al. (2014) the freezing height of the glaciers might have dropped several hundred metres in the Venezuelan Andes during the LIA, compared to the warmer phases before and after this prominent cooling episode. A warm MCA is also indicated by a peat bog in the Páramo de Piedras Blancas (site 4) in the same mountain massif. Rull and Schubert (1989) documented here a marked increase in Montane Forest and non-herbaceous Páramo indicator pollen during the period 700-1300 AD, indicating a rise, i.e. upslope shift, of the tree line (Figs. S1, S2). The two pollen groups decrease during the subsequent LIA and are replaced by Cyperaceae, suggesting very scarce regional vegetation around the site.

MCA warming is also documented in five cores from lakes and wetlands in the Andes of Colombia and Ecuador. In the Llano Grande peatbog (site 7) Velásquez-Ruiz and Hooghiemstra (2013) documented generally high concentrations of *Quercus*, representing Andean forest, during the period 500-1400 AD. Pollen of the higher elevation vegetation zones Subparamo and Paramo were reduced during the MCA, pointing to an upslope rise in the upper forest line (UFL). Similar MCA upslope shifts in the UFL have been reported from the El Triunfo wetland (site 8, Giraldo-Giraldo et al., 2018) and the Guandera peat bog (site 11, Moscol Olivera and Hooghiemstra, 2010) (Figs. S3, S4). An upward shift of the forest vegetation belt has also occurred in the Lagunas de Mojanda complex, as evidenced by an increase of pollen associated with the Lower Montane Rainforest during the period 500-1350 AD (site 12, Villota et al., 2017). Likewise, MCA temperatures were elevated at Laguna Pindo (site 13), as indicated by a temperature reconstruction based on locally calibrated chironomids (Matthews-Bird et al., 2016). Significant cooling commenced after 1600 AD during the LIA.

The MCA temperature signal of three other sites of the region is more ambiguous and deviates from the general regional trend. Bixler (2012) presented a temperature reconstruction based on distributions of branched Glycerol Dialkyl Glycerol Tetraethers (brGDGTs) in a sediment core from Laguna Chingaza (site 9) which is located 180 km ESE of site 8. According to his reconstruction, temperatures were only midly elevated during the period 1000-1200 AD, and significantly cooler than parts of the LIA and Current Warm Period (Fig. S4). However, such results have to be treated with caution because the geochemical method employed has further evolved since then and issues have been identified (see Text S2 in Supplement for details). Laguna La Cocha (site 10) lies 85 km NE of site 11 and suggests a cold MCA (Fig. S4). González-Carranza et al. (2012) based their temperature estimation on vegetation belts and the percentage of arboreal pollen which, however, may have been also influenced by human activities or changes in rainfall. Furthermore, an upward or downward shift in the age model by 200 years would place the MCA in a warm period. Finally, Jantz and Behling (2012) reported a cold spike during the MCA in the Tres Lagunas region (site 14), which lies 220 km SW of site 13, based on an abundance peak in *Isoetes* and Poaceae (Fig. S5). The authors associate this cooling explicitly with the LIA, possibly pointing to age model issues (see Supplement Text S2 for detailed discussion on all three locations). Considering the proximity to the other sites and their characteristic MCA warming pattern, we recommend re-study of sites 9, 10 and 14 with refined proxy methodology and improved chronology.

Off Peru & northern Chile and Galapagos Islands

Cores M772-056 and M772-059 were taken in the Peru upwelling zone (Nürnberg et al., 2015; Seillès et al., 2016) (Figs. 2, 4, S3). The MCA appears to have been generally cold, followed by warmer SST commencing 1200 AD (Fig. S5). Upwelling seems to have been intensified during the MCA and reduced during the LIA. The trend is somewhat reversed for the subsurface ocean temperature in 200 m water depth at this site which shows a warm subSST MCA, followed by a cold subSST LIA (Fig. S5). Influx of cold subsurface water was reduced during the MCA as the eastward-flowing Equatorial Undercurrent weakened (Nürnberg et al., 2015). Emplacement of warmer tropical waters appears to have led to the observed MCA warming of the subsurface waters in the Gulf of Guayaquil.

Marine core G10 (site 23) is located in the southern part of the Peruvian upwelling zone (Fig. 4). Also here, upwelling increased during the MCA as evidenced by more intense water column denitrification and higher oxygen-deficiency (Salvatteci et al., 2016) (Fig. S8). Similar trends were observed in the aseasonal upwelling zone of northern Chile in a marine core in Inglesa Bay (site 31). Castillo et al. (2017) documented generally cooler SST, more frequent anoxic sediment conditions and a higher biological productivity for the MCA at this location (Figs. 4, S10).

The only Pacific marine core in northern South America that lies outside upwelling systems is KNR195-5 MC42C (site 18) (Rustic et al., 2015). This core is located on the eastern side of the Galapagos Archipelago which is largely unaffected by upwelling (Fig. 4). Foraminiferal Mg/Ca-derived SST data show a warm MCA, followed by a mostly cold LIA and warm CWP (Fig. S5). The MCA temperature development of this core may be the best available and most representative for the tropical Pacific off South America. Even though modern SSTs are the highest of the millennium, yet they are within error of peak MCA values and thus are not unprecedented (Rustic et al., 2015). Sites 15, 16, 23 and 31 also yield important data, which however are spatially characteristic only for the narrow Peruvian and northern Chilean coastal upwelling belt. Note that the much-cited SST reconstruction from the El Junco volcanic crater lake (site 17) from the eastern Galapagos Archipelago (Conroy et al., 2008) primarily represents a lake water level reconstruction, hence delivers hydroclimatic information in the first place. The assumed relationship between precipitation and temperature may be temporally and spatially too complex to allow an SST interpretation for a well-defined sea area based on these data (for details see Supplement Text S2). If taken at face value, the cold MCA SST anomaly suggested by the El Junco data may refer to the intensified Peruvian upwelling where a lot of the moisture may have come from via easterly trade winds.

Central Andes

This Andean area comprises Peru, Bolivia and central Chile. MCA palaeoclimate studies from this region focus on three different proxy families: 1) Concentration of organic matter and other biological components reflecting lake and agricultural productivity which typically increases in high altitude areas under warmer conditions; 2) proxies tracking glacier retreats and advances; and 3) stable oxygen and deuterium isotopes in ice cores.

Andean MCA productivity boost

Elevated amounts of organic matter were found in the MCA section of two lakes in the southern Peruvian Cordillera Central, Tarn Challpacocha (site 25) and Tarn Yanacocha (site 28) indicating MCA warming (Stroup et al., 2015) (Fig. S8). Warm MCA temperatures also allowed high altitude agriculture in the Marcacocha lake area (site 24) as reflected by an abundance peak of Chenopodiaceae which has been - and still is - an important component of the Andean diet (Chepstow-Lusty et al., 2009) (Fig. S8). Likewise, Laguna Aculeo (site 33) in central Chile during the MCA saw an increase in chlorophyll that is primarily from autochthonous primary productivity (von Gunten et al., 2012) (Fig. S10). This is thought to be predominantly an effect of temperature on the duration of the ice-free period and the productive season.

Reduced MCA glacier activity

In the central Peruvian Cordillera Blanca Stansell et al. (2013) studied the geochemical elemental composition of three high altitude lakes that reflect changes in the extent of climate-mediated up-valley ice cover, Laguna Queshquecocha (site 20), Laguna Jahuacocha (site 21), and Laguna Lutacocha (site 22). The MCA was characterized by generally low clastic input during the MCA which is interpreted as a glacier retreat phase with lower amounts of erosional detritus (Fig. S7). ^{10}Be moraine age dating in the Qori Kalis outlet glacier in the southern Peruvian Cordillera Central (site 26) shows that the glacier was short throughout the MCA and commenced to advance sometime after the MCA, possibly around 1200 AD (Stroup et al., 2014). The glacier reached its maximum downslope extent during the period 1400-1650 AD which corresponds to the LIA.

Ice cores

Four tropical ice core sites have been studied in South America that include the MCA interval. These are the Peruvian Huascarán (site 19) and Quelccaya (site 27) ice cores, as well as the Bolivian Nevado Illimani (site 29) and Nevado Sajama (site 30) ice cores. The MCA is typically characterized by more positive $\delta^{18}O$ and δD values, which have been traditionally interpreted as reflecting warming (Ramirez et al., 2003; Thompson et al., 2003; Thompson et al., 1995; Thompson et al., 2013) (Figs. S7, S8, S10). The isotopes most likely reflect changes in the cloud top temperatures at the mean level of condensation of precipitation, rather than surface temperatures (pers. comm. Lonnie Thompson, March 2018). A warm MCA is also suggested for the Nevado Illimani ice core by an ammonium anomaly in the ice core which Kellerhals et al. (2010) interpreted as a proxy for temperature in the Amazon Basin. The overall pattern of a warm MCA, cold LIA and modern CWP warming that is documented by many non-ice-core proxies in South America is replicated in all four cores (Figs. S7, S8, S10). This gives confidence that the oxygen and deuterium isotopes may indeed to some extent represent temperature proxies. The Nevado Sajama ice core is an exception in that the modern warming is only poorly reflected by the stable oxygen isotopes. Thompson et al. (2003) suggested that the temperature signal may be mixed with an additional hydroclimate component here due to the extreme dryness of the region associated with the proximity to the Atacama Desert.

Nevertheless, the validity of $\delta^{18}O$ and δD as temperature proxies is still a matter of scientific debate. Several authors consider that deuterium and oxygen isotopes of the tropical South American ice cores reflect changes in precipitation rather than temperature (Hardy et al., 2003; Sturm et al., 2007a; Sturm et al., 2007b; Vimeux et al., 2009; Vuille and Werner, 2005). The isotope signal is thought to represent an integrated composite of precipitation over a large region along air masses pathways, instead of local precipitation in the glacier area (Villacís et al., 2008). The correlation between isotopes and local precipitation is almost zero at the interannual time-scale (pers. comm. Françoise Vimeux, April 2018). For the time being, it may be safe to assume that the ice core isotopes reflect both temperature and precipitation without fully quantifying the individual contributions. See Supplement texts S3 and S4 for detailed discussion (sites 19, 27, 29, 30).

Laguna Chepical

The only study site that deviates from the generally warm MCA pattern in the Central Andes is Laguna Chepical (site 32) in central Chile. Both clay and diatom temperature proxies suggest a cold MCA (de Jong et al., 2013; Martel-Cea et al., 2016) (Fig. S10). It is unclear whether this represents a local climate anomaly at this site or whether it results from age model issues. The sedimentation rate during the last 1000 years initially declined and then increased rapidly again after construction of a dam. A radiocarbon age data point of about 1220 AD was rejected. Therefore, major age uncertainty has to be taken into account for the MCA in Laguna Chepical, and it cannot be fully ruled out that the period of reduced summer ice recorded during the period 1150-1400 AD might in fact be 150 years older and represent the MCA itself (Fig. S10). For detailed discussion see Supplement Text S4.

Patagonia

Patagonia has the greatest density of MCA studies on the South American continent with a total of 30 land and marine sites based on a diverse set of proxy types (Fig. 2). The vast majority of the sites document a warm MCA (Figs. 4, S11-S17).

<u>*Marine*</u>

The majority of Patagonian marine cores of the main coast and in fjords have been studied by means of Uk'37 alkenone SST (sites 38, 40, 41, 50, 51, 54, 59 and 61). The temperature reconstruction of two sites is based on stable oxygen isotopes, namely of the planktic foraminifer *Globigerina bulloides* (site 43) and of *Mytilus edulis* shells (site 62). In one case chlorine was taken as a proxy to distinguish between sea water and fresh water in an area where glaciers are thought to cut-off fjords from marine influence during ice advance phases (site 62).

All sites suggest climatic warming during the MCA, except two. One of the exceptions is core GeoB 7186-3 off Chile (site 40) where Mohtadi et al. (2007) inferred a long-term cooling trend over the past 1400 years, rather than the regionally characteristic centennial-scale climatic fluctuations. As this appears to be an outlier, it may be worth re-studying this location with an additional core and/or complementary methodology. Higher resolving data are needed for core CHURR in the Churruca fjord, western Strait of Magellan (site 54). Caniupán et al. (2014) published a Uk'37 SST dataset which suggests warming during the period 500-1100 AD, followed by cooling (Fig. S10). However, it cannot be excluded that the second half of the MCA here was also warm, because the only cold data point is dated as 1200 AD, after the MCA had ended. Even though the Patagonian Pacific coast lies in an upwelling zone, the predominantly warm nature of the MCA here indicates that SST is dominated by regional climate, rather than changes in upwelling. This may be due to the seasonally restricted upwelling, whilst in Peru it occurs year-round.

Core GeoB 3313-1 suggests a southward shift of the Westerlies during the MCA, as indicated by an increase in iron content in the sediment (Lamy et al., 2002). Latitudinal shifts of the Southern Westerly Winds have been identified as a key driver to Holocene climatic and oceanographic changes in Patagonia and central Chile (Jenny et al., 2002; Kaplan et al., 2016; Mohtadi et al., 2007; Sepúlveda et al., 2009).

Lakes and Wetlands

The MCA in Patagonia and Tierra del Fuego has been studied in five lakes and one wetland using diverse methodologies. These include duration of the cold season ice cover based on depositional rates (Laguna San Pedro, site 34), biogenic silica as biological productivity indicator (Laguna Escondida, site 42; Laguna Las Vizcachas, site 52), summer layer thickness in varves (Lago Plomo, site 45), intensity of meltwater flux and change in clastic source terrain (Lago del Desierto, site 47), and *Nothofagus* pollen abundance at its southern distribution limit (Isla de los Estados, site 63) (Figs. S12-S17). All results point to a warm MCA. This is also supported by age-at-death profiles of hunter-gatherers in Southern Patagonia (Suby et al., 2017). Life appears to have been easier under warmer conditions as the population percentage of people reaching the age 35-50 years nearly halved from the MCA to the LIA, from 25% to 14%.

<u>Glacier Moraine Dating</u>

Moraine ages have been determined in various glaciers of Patagonia and Tiera del Fuego based on radiocarbon and dendrochronological dating of trees (Soler Glacier, site 44; Glaciar Jorge Montt, site 46; Glaciar Lengua, site 56), ^{10}Be moraine ages (Herminita Peninsula, site 48) and other radiocarbon or integrated techniques (Patagonian Icefield synthesis, site 49; Tyndall Glacier, site 53; Seno Skyring Glacier lobe, site 57; Ema Glacier, site 60). All studies point to a warm MCA with shortened glaciers (Text S5; Figs. S15, S17). Glaciers re-advanced a few decades after 1200 AD when the MCA ended.

<u>Tree Rings</u>

Four tree rings sites have been described in the literature from the greater Patagonian region that reach back to the MCA. Three sites are based on *Fitzroya cupressoides* (Rio Alerce, site 36; Costa del Osorno, site 37; Abtao, site 39), and one refers to *Araucaria araucana* (Captren, site 35). Three of the sites (Captren, Rio Alerce and Abtao) show a clear warming signal for the MCA (Fig. S12). The trend in Costa del Osorno is unclear with intermediate ring thicknesses during the MCA.

<u>Caves</u>

At the Marcelo Arevalo cave (site 55), Mühlinghaus et al. (2008) reconstructed temperatures of two stalagmites using a Combined Stalagmite Model (CSM) that is based on $\delta^{13}C$ and $\delta^{18}O$ profiles along the growth axis. The authors documented a warm phase for the MCA (Fig. S16).

Atlantic Margin and South American Plains

<u>*Marine*</u>

Six marine MCA cores have been studied from the South American Atlantic margin. SST have been reconstructed based on planktonic foraminifera assemblages for core GS07-150 17/2 in the Potiguar Basin (site 64), and based on the Mg/Ca ratio of *Globigerinoides ruber* (white, sensu stricto) for core GeoB6211 off southernmost Brazil (site 69). Both sites are located outside upwelling zones and show a warm MCA that probably represents regional MCA oceanic warming (Fig. S19). Sites 66-68 are located in the Cabo Frio and South Brazil Bight upwelling zone of the Santos Basin (Palma and Matano, 2009) (Fig. 4). Planktonic foraminifera have been studied as upwelling markers and SST assemblages (Lessa et al., 2016; Pivel et al., 2013; Souto et al., 2011) and document a cold MCA with intensified upwelling of South Atlantic Central Water (SACW) (Fig. S19).

Core GeoB13862-1 (site 76) from the Mar del Plata Canyon in northern Argentina indicates a southward shift of the Brazil-Malvinas Confluence (BMC) and of the westerly winds as well as progressive strengthening of the Antarctic Intermediate Water during the MCA, based on oxygen isotopes of the planktonic foraminifer *Globorotalia inflata* and sortable silt (Voigt et al., 2016; Voigt et al., 2015) (Fig. S20). The southward shift of the BMC might have also intensified the formation of South Atlantic Central Water (SACW) that is then transported counter-clockwise through the South Atlantic Subtropical Gyre to Cabo Frio where it forms the source of the upwelling waters (Coelho-Souza et al., 2012; Souto et al., 2011). Stronger SACW transport onto the Cabo Frio shelf during the MCA might have resulted in increased upwelling and biological productivity in the Brazilian upwelling zones.

Land

A peatland study from the Brazilian state of Minas Gerais (site 65) based on plant composition changes suggests a warm and wet MCA (Schellekens et al., 2014). A warm MCA is also indicated in four lake studies in coastal Uruguay and the Argentinian Pampas. Temperature reconstruction in Pena Lagoon (site 70) and Laguna Blanca (site 71) in Uruguay are interpreted from opal phytoliths (del Puerto et al., 2013; del Puerto et al., 2006), whilst Laguna Nassau (site 74) and Lake Lonkoy (site 75) in the Argentinian Pampas were studied by means of palynology (Stutz et al., 2012; Vilanova et al., 2015) (Fig. S20). MCA warming is also suggested by two regional analyses of the South American Plains (listed here as sites 72 and 73). More robust methodologies are needed to better understand the late Holocene temperature changes in the South American regions outside the Andes, e.g. geochemical biomarkers, in order to close these data gaps.

Summary of MCA trends in South America

The vast majority of all South American sites suggest a warm MCA (Fig. 4). Andean vegetation zones moved upslope, glaciers retreated, biological productivity in high altitude lakes increased, the duration of cold season ice cover on Andean lakes shortened, and trees produced thicker annual rings. Sea surface temperatures of non-upwelling regions were generally elevated during the MCA. The same trend is found in some seasonal upwelling zones such as the Southern Caribbean and Pacific Patagonian upwelling systems where the regional warming signal appears to dominate the reconstructed SST values. In contrast, MCA cooling associated with intensified upwelling productivity occurred in the year-round Peruvian upwelling system, as well as in the seasonal Brazilian Cabo Frio and northern Chilean upwelling zones. Most of the MCA cooling documented in the literature so far is restricted to these spatially limited high productivity systems. A few exceptions exist on land, which either represent local MCA anomalies or have issues related to age model, proxy methodology or anthropogenic landuse activities. MCA studies indicate that some of the key climatic elements of South American have shifted during the MCA. The westerly winds and the Brazil / Malvinas Confluence (BMC) appear to have shifted southwards, whilst the ITCZ shifted northwards (Fig. 4). The Pacific Equatorial Undercurrent weakened and the South Atlantic Central Water strengthened.

The integration of all available different methodologies helps to draw a more robust palaeoclimatic picture than by relying on just selected data types. A typical challenge is the differentiation between temperature and precipitation effects on climate proxies, e.g. in ice cores, glacier length variations, tree rings and pollen assemblages. Comparison between these proxies as well as with proxies that are less affected by precipitation (e.g. non-upwelling SST data) helps to make the regional palaeoclimatic picture more reliable. Unfortunately, there are still large regional data gaps. Only few MCA studies exist for the South American continental interior outside the Andes and for the Atlantic margin. The Guyanas, onshore Brazil and Paraguay are essentially unstudied in terms of medieval temperature development. This turns about half of the continent into 'palaeoclimatic white space' which requires intense future study. Indirect evidence from the Bolivian Nevado Illimani ice core (site 29) suggests MCA warming also for the Amazon Basin. The analyzed ice core ammonium is thought to have originated from here as temperature-dependent soil and vegetation emissions.

Climate Drivers

The documented MCA temperature change in South America occurred in pre-industrial times and therefore requires suitable climate drivers other than anthropogenic greenhouse gasses. A good starting point is the study of ocean cycles which are responsible for modern climate variability (e.g. Flantua et al., 2016). South American climate is heavily influenced by El Niño-Southern Oscillation (ENSO), Southern Annular Mode (SAM), and Pacific Decadal

Oscillation (PDO) (e.g. Flantua et al., 2016; Garreaud et al., 2009; Jomelli et al., 2009; Martin et al., 1993; Moy et al., 2009; Stansell et al., 2013; Villalba, 1994; Wills et al., 2018). These ocean cycles operate on a wide range of time scales starting from yearly and reaching to multicentennial. On the Atlantic side the Atlantic Multidecadal Oscillation (AMO) is a good candidate as climate driver (e.g. Baker et al., 2001). The various ocean cycles are partly interlinked (Wyatt and Curry, 2014).

ENSO

The El Niño-Southern Oscillation (ENSO) is a naturally occurring phenomenon in which ocean temperatures in the equatorial Pacific fluctuate between two states: warmer than normal central and eastern equatorial Pacific sea surface temperatures (El Niño) and cooler than normal central and eastern equatorial Pacific sea surface temperatures (La Niña). Typically, sea surface temperatures (SSTs) are used to identify the ENSO oscillation. During El Niño, Peru upwelling typically is reduced and SST increase. According to the majority of ENSO reconstructions, the MCA was characterized by more El Niño-dominated conditions (Conroy et al., 2010; Conroy et al., 2008; Henke et al., 2017; Moy et al., 2002; Rustic et al., 2015; Yan et al., 2011) (Figs. 5, 6). The Walker Circulation appears to have been weaker or reversed during the MCA.

In contrast to interannual El Niño events, the interdecadal ENSO development leads to different oceanographic changes. According to Vargas et al. (2007), interdecadal El Niño-dominated conditions, associated with a generally warm Pacific, favor the intensification of southerly winds that boost coastal upwelling and productivity along the Peruvian Chilean coast. This mechanism fits well with the MCA cooling documented for this upwelling system (sites 15, 16, 23, 31) and the proposed El Niño-dominated interdecadal ENSO of the MCA. Recent intensification of upwelling over the past few decades (Gutiérrez et al., 2011; Narayan et al., 2010) coincides with the present-day El Niño-dominated interdecadal ENSO phase (Figs. 5, 6).

During interannual El Niño events, the upwelling-favorable winds also increase but are compensated by a shoreward geostrophic near-surface current. Thermocline and nutricline deepen significantly, reducing nutrient content which, along with a mixed layer depth increase, impact the phytoplankton growth (Espinoza-Morriberón et al., 2017). Note, that other groups have previously suggested a more La Niña-dominated MCA (Cobb et al., 2003; Khider et al., 2011; Mann et al., 2009) (Fig. S1).

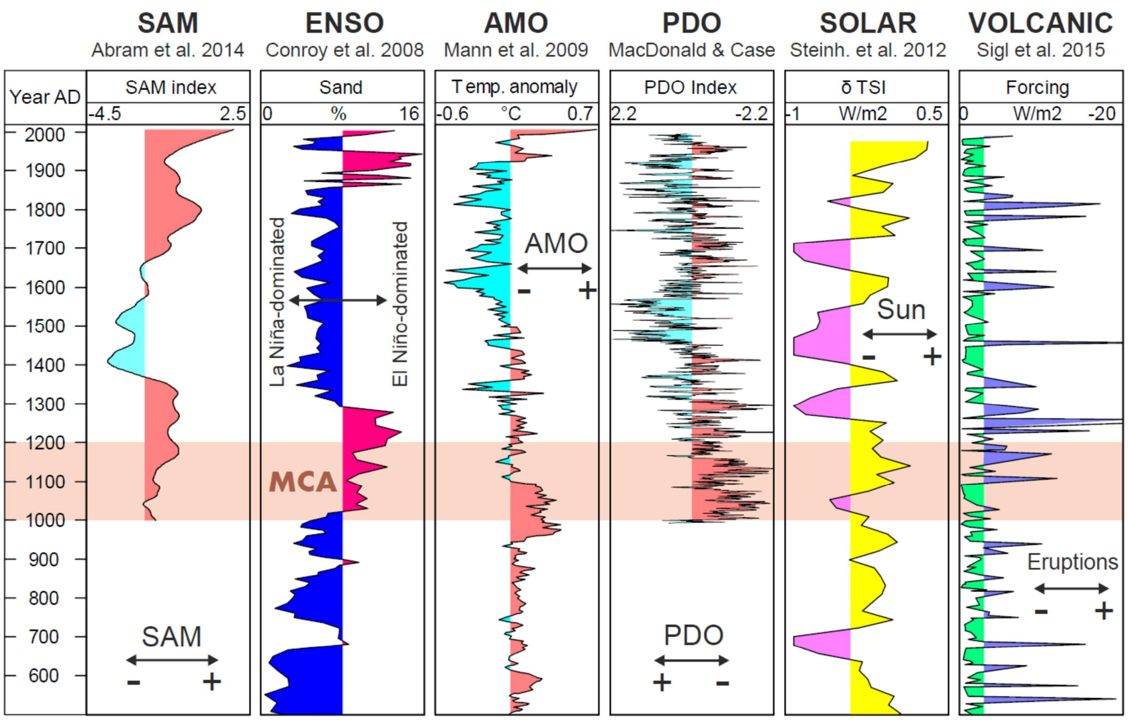

Fig. 5. *Reconstructions of key drivers of natural climate variability. Southern Annular Mode, SAM, 70 year loess filter (Abram et al., 2014); El Niño-Southern Oscillation, ENSO (Conroy et al., 2008); Atlantic Multidecadal Oscillation, AMO (Mann et al., 2009); Pacific Decadal Oscillation, PDO (MacDonald and Case, 2005); solar activity changes (Steinhilber et al., 2012); volcanic eruptions (Sigl et al., 2015).*

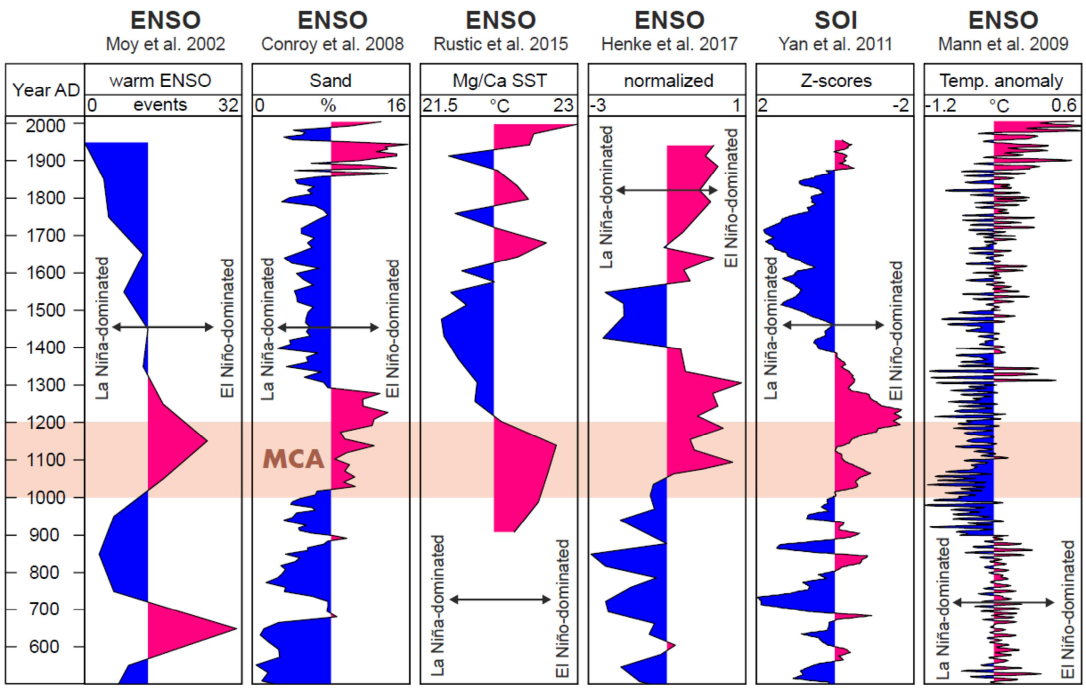

Fig. 6. *Changes in El Niño-Southern Oscillation (ENSO) during the past 1500 years according to different reconstructions (Conroy et al., 2008; Henke et al., 2017: temperature ensemble; Mann et al., 2009; Moy et al., 2002; Rustic et al., 2015; Yan et al., 2011)*

<u>SAM</u>

The Southern Annular Mode (SAM) is also known as Antarctic Oscillation (AAO) and forms a low-frequency mode of atmospheric variability of the SH (e.g. Ekaykin et al., 2017; Gillett et al., 2006). The SAM is measured as atmospheric pressure difference between subpolar high latitudes (lower pressure) and subtropical mid latitudes (higher pressures), and describes the north-south movement of the westerly wind belt that circles Antarctica. In its positive phase (SAM+), the westerly wind belt shifts towards Antarctica and strengthens, while in its negative phase the belt moves towards the Equator (Liau and Chao, 2017). The ocean cycle has a marked influence on eastern Pacific SST (e.g. Ancapichun and Garces-Vargas, 2015). SAM reconstructions for the past 1000 years illustrate a general tripartition. Between 1000 and 1350 AD the SAM fluctuated around a neutral (or slightly negative) level, followed by a pronounced negative phase 1350-1700 AD during the LIA and a more positive phase since 1700 AD (Abram et al., 2014; Dätwyler et al., 2017; Hessl et al., 2017; Huang et al., 2010) (Fig. 5). The strongest positive SAM type circulation that is similar to the past few decades may have occurred during 1100-1220 AD (Goodwin et al., 2014).

PDO

The Pacific Decadal Oscillation (PDO) is an ocean cycle based on switching ocean temperature anomalies in the northeast and tropical Pacific Ocean. When SSTs are anomalously cool in the interior North Pacific and warm along the eastern Pacific Coast, the PDO has a positive value. When these climate anomaly patterns are reversed the PDO has a negative value. Andean climate and east Pacific upwelling are influenced by the PDO (e.g. Ancapichun and Garces-Vargas, 2015; Castillo et al., 2017; Elbert et al., 2013a; Veettil et al., 2017; Vuille et al., 2015). A PDO reconstruction by MacDonald and Case (2005) suggests a negative PDO phase for the MCA.

AMO

The Atlantic Multidecadal Oscillation (AMO) is an ocean cycle with an estimated period of 60-80 years that is based upon the average anomalies of SST in the North Atlantic basin, 0-80°N. The AMO influences South American climate in various ways (e.g. Kayano and Capistrano, 2014; Martínez et al., 2015). A reconstruction by Mann et al. (2009) shows that the AMO has been positive during the MCA and CWP and negative during the LIA (Fig. 5). South American temperature development of the past 1500 years shows a surprisingly high degree of similarity to the AMO changes. The AMO has been documented to modulate South American summer monsoon activity and therefore rainfall in northeastern Brazil (Novello et al., 2012) and the northwestern Amazon Basin (Apaéstegui et al., 2014) during the past few millennia.

Solar Activity Changes

Solar activity varied during the past millennia, as reconstructed based on cosmic-ray produced radionuclides, such as ^{10}Be and ^{14}C which are stored in polar ice cores and tree rings (Lean, 2018; Muscheler et al., 2016; Steinhilber et al., 2012; Usoskin et al., 2016). The MCA is characterized by generally high solar activity that lasted from 725-1250 AD, except for the brief Oort Minimum at the beginning of the MCA at 1010-1050 AD (Fig. 5). Solar activity and ocean cycles show several similarities in their development. Most ocean cycles turned positive during the solar-active MCA, except the PDO which appears generally inverted compared to the others (Fig. 5). During the subsequent LIA, solar activity decreased and most ocean cycles turned negative. When studied in detail, characteristic time lags and patterns exist for the different ocean cycles.

The physical processes that may link solar activity, ocean cycles and climate are still very much unclear but are being actively researched (e.g. Arblaster and Meehl, 2006; Hassan et al., 2016; Kuroda and Kodera, 2005; Li and Xiao, 2018; Mehta and Lau, 1997; Nuzhdina, 2002; Roy and Haigh, 2011; Salas et al., 2016; Yan et al., 2011). Nevertheless, a large amount of empirical evidence has been published which suggests a significant solar-forced component in South American climate. Timing of several LIA glacier advance phases in the Venezuelan and Bolivian Andes coincides well with solar minima (Polissar et al., 2006; Rabatel et al., 2005). SH Westerly Winds typically shift southwards during of higher solar activity and show a 250 year periodicity that falls into the solar Suess-de Vries cycle (Turney et al., 2016; Varma et al., 2011; Varma et al., 2012). Circulation in the western tropical South Atlantic and South American tropical rainfall show multi-centennial to millennial oscillations that are associated with typical solar cyclicities (Baker et al., 2005; Chiessi et al., 2014; Novello et al., 2016; Santos et al., 2013; Stríkis et al., 2011). Prominent solar minima have resulted in major hydroclimatic disruptions on the continent and are interpreted to have shifted the ITCZ southwards, possibly affecting the Atlantic Meridian Overturning Circulation

(Chambers et al., 2014; Moreira-Turcq et al., 2014). The 11 and 22 years Schwabe and Hale solar cycles have been found in South American palaeohydroclimatic archives (Black et al., 2004; Gusev and Martin, 2012; Heredia and Elias, 2013; Hernández et al., 2010; Mauas et al., 2011), as well as in tree rings (Nordemann et al., 2005; Perone et al., 2016; Prestes et al., 2011; Rigozo et al., 2008a; Rigozo et al., 2007; Rigozo et al., 2008b).

Variability in the Peru-Chile upwelling appears also to be influenced by solar activity changes, especially by the solar Gleissberg cycles with a periodicity of 80-100 years (Agnihotri et al., 2008; Guiñez et al., 2014). Higher solar activity is thought to shift the Westerlies wind system and South Pacific High towards the south (Varma et al., 2011) which leads to an intensification of upwelling (Salvatteci et al., 2014; Salvatteci et al., 2016). Likewise, a recent southward displacement of the South Pacific High during the beginning of the 21st century resulted in stronger upwelling and water column cooling over the continental shelf off central-south Chile (Ancapichun and Garces-Vargas, 2015; Schneider et al., 2017).

Volcanism

The reconstructions of global volcanic forcing (Sigl et al., 2015) and global volcanic aerosol optical depth (Crowley and Unterman, 2013) suggest low volcanic activity during the early part of the MCA (950-1100 AD), and increased volcanic activity in the second half (1100-1350 AD), followed by low volcanic activity (1350-1600 AD) (Fig. 5). Comparison with South American temperature proxy records does not reveal a climate signal in the MCA and early LIA climate data that would correspond to this global volcanic activity pattern.

South America in continent-wide and global temperature reconstructions

The best existing temperature reconstruction published for South America covering the last millennium comes from by Neukom et al. (2011). In their reconstruction of summer temperatures, that is spatially restricted to southern South America, the period 900-1350 AD showed significantly elevated values that even partly exceeded modern levels (Fig. 3). Notably, the later part of the MCA appears rather cold which may be due to local fluctuation at one of the two used proxy records, Laguna Aculeo (site 33). The majority of all other MCA records from South America do not show such a marked late MCA cold episode (Figs. S2-S20). Future continent-wide reconstructions will have the benefit to use a much greater number of sites which will help to average out such local effects. Several records used in previous SH temperature reconstructions have meanwhile turned out to be more likely hydroclimate proxies. For example, Mann et al. (2008) included the Ecuadorian Lake Pallcacocha (Moy et al., 2002), whilst Neukom et al. (2014) added the three Peruvian sites Cascayunga Cave (Bird et al., 2011b; Reuter et al., 2009), Laguna Pumacocha (Bird et al., 2011a; Bird et al., 2011b) and marine core CO147-106KL (Rein et al., 2004; Salvatteci et al., 2014). The MCA temperature anomaly map published by Mann et al. (2009: their fig. 2) needs to be treated with caution, as it is unclear how such a detailed temperature anomaly pattern can be deduced from just two proxy series (Quelccaya ice core and Lake Pallcacocha). Furthermore, both records may actually represent hydroclimate proxies rather than temperature series.

The latest South America temperature reconstruction by the PAGES 2k Consortium (2013) suggests a significant delay of MCA warming that commences only around 1200 AD. This appears to be mostly related to one of the two used proxy records, Laguna Aculeo (site 33) which is not fully characteristic for the continent-wide MCA temperature development, neither matches with the Andean glacial activity data that sees an earlier onset of warming and a return to cooling after 1200 AD. Meanwhile, the PAGES 2k Consortium (2017) has updated its proxy database and added the two Chilean sites Laguna Escondida (our site 42) and

Laguna Chepical (our site 32). Whilst Laguna Escondida matches well with the regional MCA development, Laguna Chepical shows a rare cold MCA and therefore appears to be representative for only a small area. Nearby Laguna Aculeo (site 33) already displays a much warmer MCA (Figs. 3, S10). Future composite temperature curves will have to take areal representativeness into account when weighting the various proxies.

Conclusions

The vast majority of all 76 studied South American land and marine sites suggest a warm MCA. An exception are the year-round upwelling zones of Peru, northern Chile and Cabo Frio (Brazil) where upwelling intensified during the MCA due to changes in winds and ocean currents. MCA warming in South America and the NH appears to have occurred largely synchronous, probably reaching comparable intensities. The MCA climate map provides important input data to climate models which are now tasked to replicate the observed MCA climate patterns and their possible natural climatic drivers, i.e. multi-centennial Pacific and Atlantic ocean cycles and changes in solar activity.

As is typical for such a data review, occasional issues with data resolution, robustness of age models and validity of temperature proxies have been identified. These are discussed in detail in the site descriptions of the Supplement to this paper. Several perceived outlier sites may warrant a re-study with the objective to reproduce the age model and add independent complementary temperature proxy types. A fully quantitative comparison of MCA and CWP temperatures is still complicated. Some sites suggest that the CWP may have been warmer than the MCA, whilst others indicate the opposite. In yet other sites, the two warm phases reached a similar temperature level. Part of these discrepancies may be attributable to regional variations across the continent, whilst another part may be due to incompletely understood proxies. Further studies are needed to investigate competing influences of temperature and precipitation changes on key climate archives and proxies such as ice cores, palynology, tree rings, speleothems, marine cores and lake records.

The majority of MCA publications focus on the high altitude Andean mountain belt. Data from regions outside the Andes are still scarce, especially from the central and eastern parts of South America. Concerted research efforts are needed to document the MCA climate history of these areas. Palaeoclimate proxy methodologies need to be developed and tested that are effective in these lower altitude settings, e.g. biomarker-based lake palaeotemperature reconstructions. Multi-proxy based research should become a mandatory strategy for all further investigations (Flantua et al., 2016). Future quantitative temperature reconstructions for South America need to diversify their regional data basis, as existing composites still depend on too few MCA sites which then introduce local bias.

Acknowledgements

We wish to thank all scientists whose case studies form the basis of this palaeoclimate mapping synthesis. We are grateful for provision of tabulated data and valuable discussions to Guillaume Leduc, Philippe Martinez, Juan Federico Ponce, Alexis Castillo, Hermann Behling, Henry Hooghiemstra, Renato Salvatteci, Giuseppe Siani, Ana Luiza Albuquerque, Ricardo Villalba, Lucien von Gunten, Frank Bosse, Laura Scafati, Lonnie Thompson, Mariza Pereira de Souza Echer, Nora Irene Maidana, Isabel Vilanova, Jorge Strelin, Judith Schellekens, Nathan Stansell, Bernd Zolitschka, Françoise Vimeux, Jessica Conroy, Gerald Rustic, and Gabriel Vargas Easton. A large amount of data were sourced through the PANGAEA online data base and the NOAA National Centers for Environmental Information (NCEI, formerly NCDC), invaluable services which are greatly acknowledged. We are indebted to Jurgis Klaudius and Lloyd’s Register for kindly providing the database and correlation software IC™ for this project. This review forms part of the Medieval Climate Anomaly Mapping Project which has been kindly supported by crowdfunding. We are particularly grateful to Jens Kröger for helping to jump-start the project. Note that this study is fully unrelated to the first author’s employment in the hydrocarbon sector and was neither commissioned nor funded by the energy industry. SL undertook this study outside office hours as a private person, trained geoscientist, and former full-time academic. The project was greatly facilitated by Google My Maps which allows to effectively capture and share MCA map data with the climate science community. The vectorised South American base map in this paper was sourced from http://www.d-maps.com, a useful service for which we are thankful. We are grateful to two anonymous reviewers who greatly helped to improve this manuscript.

References

Abram, N. J., Mulvaney, R., Vimeux, F., Phipps, S. J., Turner, J., and England, M. H., 2014, Evolution of the Southern Annular Mode during the past millennium: Nature Climate Change, v. 4, p. 564.

Agnihotri, R., Altabet, M. A., Herbert, T. D., and Tierney, J. E., 2008, Subdecadally resolved paleoceanography of the Peru margin during the last two millennia: Geochemistry, Geophysics, Geosystems, v. 9, no. 5.

Aguilar, E., Peterson, T. C., Obando, P. R., Frutos, R., Retana, J. A., Solera, M., Soley, J., García, I. G., Araujo, R. M., Santos, A. R., Valle, V. E., Brunet, M., Aguilar, L., Álvarez, L., Bautista, M., Castañón, C., Herrera, L., Ruano, E., Sinay, J. J., Sánchez, E., Oviedo, G. I. H., Obed, F., Salgado, J. E., Vázquez, J. L., Baca, M., Gutiérrez, M., Centella, C., Espinosa, J., Martínez, D., Olmedo, B., Espinoza, C. E. O., Núñez, R., Haylock, M., Benavides, H., and Mayorga, R., 2005, Changes in precipitation and temperature extremes in Central America and northern South America, 1961–2003: Journal of Geophysical Research: Atmospheres, v. 110, no. D23.

Aguilera-Betti, I., Muñoz, A. A., Stahle, D., Figueroa, G., Duarte, F., González-Reyes, Á., Christie, D., Lara, A., González, M. E., Sheppard, P. R., Sauchyn, D., Moreira-Muñoz, A., Toledo-Guerrero, I., Olea, M., Apaz, P., and Fernandez, A., 2017, The First Millennium-Age Araucaria Araucana in Patagonia: Tree-Ring Research, v. 73, no. 1, p. 53-56.

Ancapichun, S., and Garces-Vargas, J., 2015, Variability of the Southeast Pacific Subtropical Anticyclone and its impact on sea surface temperature off north-central Chile: 2015, v. 41, no. 1, p. 20.

Aniya, M., 1995, Holocene Glacial Chronology in Patagonia: Tyndall and Upsala Glaciers: Arctic and Alpine Research, v. 27, no. 4, p. 311-322.

-, 2013, Holocene glaciations of Hielo Patagónico (Patagonia Icefield), South America: A brief review: Geochemical Journal, v. 47, no. 2, p. 97-105.

Apaéstegui, J., Cruz, F. W., Sifeddine, A., Vuille, M., Espinoza, J. C., Guyot, J. L., Khodri, M., Strikis, N., Santos, R. V., Cheng, H., Edwards, L., Carvalho, E., and Santini, W., 2014, Hydroclimate variability of the northwestern Amazon Basin near the Andean foothills of Peru related to the South American Monsoon System during the last 1600 years: Clim. Past, v. 10, no. 6, p. 1967-1981.

Aracena, C., Kilian, R., Lange, C. B., Bertrand, S., Lamy, F., Arz, H. W., De Pol-Holz, R., Baeza, O., Pantoja, S., and Kissel, C., 2015, Holocene variations in productivity associated with changes in glacier activity and freshwater flux in the central basin of the Strait of Magellan: Palaeogeography, Palaeoclimatology, Palaeoecology, v. 436, p. 112-122.

Arblaster, J. M., and Meehl, G. A., 2006, Contributions of External Forcings to Southern Annular Mode Trends: Journal of Climate, v. 19, no. 12, p. 2896-2905.

Baker, P. A., Fritz, S. C., Garland, J., and Ekdahl, E., 2005, Holocene hydrologic variation at Lake Titicaca, Bolivia/Peru, and its relationship to North Atlantic climate variation: Journal of Quaternary Science, v. 20, no. 7-8, p. 655-662.

Baker, P. A., Seltzer, G. O., Fritz, S. C., Dunbar, R. B., Grove, M. J., Tapia, P. M., Cross, S. L., Rowe, H. D., and Broda, J. P., 2001, The History of South American Tropical Precipitation for the Past 25,000 Years: Science, v. 291, no. 5504, p. 640-643.

Bertrand, S., Lange, C. B., Pantoja, S., Hughen, K., Van Tornhout, E., and Wellner, J. S., 2017, Postglacial fluctuations of Cordillera Darwin glaciers (southernmost Patagonia) reconstructed from Almirantazgo fjord sediments: Quaternary Science Reviews, v. 177, p. 265-275.

Bird, B. W., Abbott, M. B., Rodbell, D. T., and Vuille, M., 2011a, Holocene tropical South American hydroclimate revealed from a decadally resolved lake sediment δ18O record: Earth and Planetary Science Letters, v. 310, no. 3, p. 192-202.

Bird, B. W., Abbott, M. B., Vuille, M., Rodbell, D. T., Stansell, N. D., and Rosenmeier, M. F., 2011b, A 2,300-year-long annually resolved record of the South American summer monsoon from the Peruvian Andes: PNAS, v. 108, no. 21, p. 8583-8588.

Bixler, C. W., 2012, A 1,500-year record of late Holocene temperature variability and recent warming from Laguna Chingaza, ColombiaMSc thesis]: University of Texas at Austin.

Black, D. E., Abahazi, M. A., Thunell, R. C., Kaplan, A., Tappa, E. J., and Peterson, L. C., 2007, An 8-century tropical Atlantic SST record from the Cariaco Basin: Baseline variability, twentieth-century warming, and Atlantic hurricane frequency: Paleoceanography, v. 22, no. 4.

Black, D. E., Peterson, L. C., Overpeck, J. T., Kaplan, A., Evans, M. N., and Kashgarian, M., 1999, Eight Centuries of North Atlantic Ocean Atmosphere Variability: Science, v. 286, no. 5445, p. 1709-1713.

Black, D. E., Thunell, R. C., Kaplan, A., Peterson, L. C., and Tappa, E. J., 2004, A 2000-year record of Caribbean and tropical North Atlantic hydrographic variability: Paleoceanography, v. 19, no. 2.

Braun, C., and Bezada, M., 2013, The History and Disappearance of Glaciers in Venezuela: Journal of Latin American Geography, v. 12, no. 2, p. 85-124.

Caniupán, M., Lamy, F., Lange, C. B., Kaiser, J., Kilian, R., Arz, H. W., León, T., Mollenhauer, G., Sandoval, S., De Pol-Holz, R., Pantoja, S., Wellner, J., and Tiedemann, R., 2014, Holocene sea-surface temperature variability in the Chilean fjord region: Quaternary Research, v. 82, no. 2, p. 342-353.

Capone, D. G., and Hutchins, D. A., 2013, Microbial biogeochemistry of coastal upwelling regimes in a changing ocean: Nature Geosci, v. 6, no. 9, p. 711-717.

Castillo, A., Valdés, J., Sifeddine, A., Reyss, J.-L., Bouloubassi, I., and Ortlieb, L., 2017, Changes in biological productivity and ocean-climatic fluctuations during the last ~1.5kyr in the Humboldt ecosystem off northern Chile (27°S): A multiproxy approach: Palaeogeography, Palaeoclimatology, Palaeoecology, v. 485, p. 798-815.

Chambers, F. M., Brain, S. A., Mauquoy, D., McCarroll, J., and Daley, T., 2014, The ‘Little Ice Age’ in the Southern Hemisphere in the context of the last 3000 years: Peat-based proxy-climate data from Tierra del Fuego: The Holocene, v. 24, no. 12, p. 1649-1656.

Chepstow-Lusty, A. J., Frogley, M. R., Bauer, B. S., Leng, M. J., Boessenkool, K. P., Carcaillet, C., Ali, A. A., and Gioda, A., 2009, Putting the rise of the Inca Empire within a climatic and land management context: Clim. Past, v. 5, no. 3, p. 375-388.

Chevallier, P., Pouyaud, B., Suarez, W., and Condom, T., 2011, Climate change threats to environment in the tropical Andes: glaciers and water resources: Regional Environmental Change, v. 11, no. 1, p. 179-187.

Chiessi, C. M., Mulitza, S., Groeneveld, J., Silva, J. B., Campos, M. C., and Gurgel, M. H. C., 2014, Variability of the Brazil Current during the late Holocene: Palaeogeography, Palaeoclimatology, Palaeoecology, v. 415, p. 28-36.

Cioccale, M. A., 1999, Climatic fluctuations in the Central Region of Argentina in the last 1000 years: Quaternary International, v. 62, no. 1, p. 35-47.

Coelho-Souza, S. A., López, M. S., Guimarães, J. R. D., Coutinho, R., and Candella, R. N., 2012, Biophysical interactions in the Cabo Frio upwelling system, southeastern Brazil: Brazilian Journal of Oceanography, v. 60, p. 353-365.

Collins, J. M., Chaves, R. R., and Marques, V. d. S., 2009, Temperature Variability over South America: Journal of Climate, v. 22, no. 22, p. 5854-5869.

Conroy, J. L., Overpeck, J. T., Cole, J. E., Shanahan, T. M., and Steinitz-Kannan, M., 2008, Holocene changes in eastern tropical Pacific climate inferred from a Galápagos lake sediment record: Quaternary Science Reviews, v. 27, no. 11, p. 1166-1180.

Conroy, J. L., Restrepo, A., Overpeck, J. T., Steinitz-Kannan, M., Cole, J. E., Bush, M. B., and Colinvaux, P. A., 2009, Unprecedented recent warming of surface temperatures in the eastern tropical Pacific Ocean: Nature Geoscience, v. 2, p. 46-50.

Crowley, T. J., and Lowery, T. S., 2000, How Warm Was the Medieval Warm Period?: AMBIO: A Journal of the Human Environment, v. 29, no. 1, p. 51-54.

Crowley, T. J., and Unterman, M. B., 2013, Technical details concerning development of a 1200 yr proxy index for global volcanism: Earth Syst. Sci. Data, v. 5, no. 1, p. 187-197.

Dätwyler, C., Neukom, R., Abram, N. J., Gallant, A. J. E., Grosjean, M., Jacques-Coper, M., Karoly, D. J., and Villalba, R., 2017, Teleconnection stationarity, variability and trends of the Southern Annular Mode (SAM) during the last millennium: Climate Dynamics.

de Jong, R., von Gunten, L., Maldonado, A., and Grosjean, M., 2013, Late Holocene summer temperatures in the central Andes reconstructed from the sediments of high-elevation Laguna Chepical, Chile (32° S): Clim. Past, v. 9, no. 4, p. 1921-1932.

del Puerto, L., Bracco, R., Inda, H., Gutiérrez, O., Panario, D., and García-Rodríguez, F., 2013, Assessing links between late Holocene climate change and paleolimnological development of Peña Lagoon using opal phytoliths, physical, and geochemical proxies: Quaternary International, v. 287, p. 89-100.

del Puerto, L., García-Rodríguez, F., Inda, H., Bracco, R., Castiñeira, C., and Adams, J. B., 2006, Paleolimnological evidence of Holocene climatic changes inLake Blanca, southern Uruguay: Journal of Paleolimnology, v. 36, no. 2, p. 151-163.

Diaz, H. F., Trigo, R., Hughes, M. K., Mann, M. E., Xoplaki, E., and Barriopedro, D., 2011, Spatial and Temporal Characteristics of Climate in Medieval Times Revisited: Bulletin of the American Meteorological Society, v. 92, no. 11, p. 1487-1500.

Ekaykin, A. A., Vladimirova, D. O., Lipenkov, V. Y., and Masson-Delmotte, V., 2017, Climatic variability in Princess Elizabeth Land (East Antarctica) over the last 350 years: Clim. Past, v. 13, no. 1, p. 61-71.

Elbert, J., Jacques-Coper, M., Van Daele, M., Urrutia, R., and Grosjean, M., 2013a, A 1500 yr warm-season temperature record from varved Lago Plomo, Northern Patagonia (47° S) and implications for the Pacific Decadal Oscillation (PDO): Clim. Past Discuss., v. 2013, p. 1771-1801.

Elbert, J., Wartenburger, R., von Gunten, L., Urrutia, R., Fischer, D., Fujak, M., Hamann, Y., Greber, N. D., and Grosjean, M., 2013b, Late Holocene air temperature variability reconstructed from the sediments of Laguna Escondida, Patagonia, Chile (45°30′S): Palaeogeography, Palaeoclimatology, Palaeoecology, v. 369, p. 482-492.

Escribano, R., and Schneider, W., 2007, The structure and functioning of the coastal upwelling system off central/southern Chile: Progress in Oceanography, v. 75, no. 3, p. 343-347.

Esper, J., and Frank, D., 2009, The IPCC on a heterogeneous Medieval Warm Period: Climatic Change, v. 94, no. 3, p. 267-273.

Espinoza-Morriberón, D., Echevin, V., Colas, F., Tam, J., Ledesma, J., Vásquez, L., and Graco, M., 2017, Impacts of El Niño events on the Peruvian upwelling system productivity: Journal of Geophysical Research: Oceans, v. 122, no. 7, p. 5423-5444.

Euler, C., and Ninnemann, U. S., 2010, Climate and Antarctic Intermediate Water coupling during the late Holocene: Geology, v. 38, no. 7, p. 647-650.

Fey, M., Korr, C., Maidana, N. I., Carrevedo, M. L., Corbella, H., Dietrich, S., Haberzettl, T., Kuhn, G., Lücke, A., Mayr, C., Ohlendorf, C., Paez, M. M., Quintana, F. A., Schäbitz, F., and Zolitschka, B., 2009, Palaeoenvironmental changes during the last 1600 years inferred from the sediment record of a cirque lake in southern Patagonia (Laguna Las Vizcachas, Argentina): Palaeogeography, Palaeoclimatology, Palaeoecology, v. 281, no. 3, p. 363-375.

Flantua, S. G. A., Hooghiemstra, H., Vuille, M., Behling, H., Carson, J. F., Gosling, W. D., Hoyos, I., Ledru, M. P., Montoya, E., Mayle, F., Maldonado, A., Rull, V., Tonello, M. S., Whitney, B. S., and González-Arango, C., 2016, Climate variability and human impact in South America during the last 2000 years: synthesis and perspectives from pollen records: Clim. Past, v. 12, no. 2, p. 483-523.

Fletcher, M.-S., and Moreno, P. I., 2012, Vegetation, climate and fire regime changes in the Andean region of southern Chile (38°S) covaried with centennial-scale climate anomalies in the tropical Pacific over the last 1500 years: Quaternary Science Reviews, v. 46, no. 0, p. 46-56.

Garreaud, R. D., Vuille, M., Compagnucci, R., and Marengo, J., 2009, Present-day South American climate: Palaeogeography, Palaeoclimatology, Palaeoecology, v. 281, no. 3, p. 180-195.

Gillett, N. P., Kell, T. D., and Jones, P. D., 2006, Regional climate impacts of the Southern Annular Mode: Geophysical Research Letters, v. 33, no. 23, p. n/a-n/a.

Giraldo-Giraldo, M. J., Velásquez-Ruiz, C. A., and Pardo-Trujillo, A., 2018, Late-Holocene pollen-based paleoenvironmental reconstruction of the El Triunfo wetland, Los Nevados National Park (Central Cordillera of Colombia): The Holocene, v. 28, no. 2, p. 183-194.

Glasser, N. F., Hambrey, M. J., and Aniya, M., 2002, An advance of Soler Glacier, North Patagonian Icefield, at c. AD 1222–1342: The Holocene, v. 12, no. 1, p. 113-120.

Goni, M. A., Woodworth, M. P., Aceves, H. L., Thunell, R. C., Tappa, E., Black, D., Müller-Karger, F., Astor, Y., and Varela, R., 2004, Generation, transport, and preservation of the alkenone-based U37K′ sea surface temperature index in the water column and sediments of the Cariaco Basin (Venezuela): Global Biogeochemical Cycles, v. 18, no. 2, p. n/a-n/a.

González-Carranza, Z., Hooghiemstra, H., and Vélez, M. I., 2012, Major altitudinal shifts in Andean vegetation on the Amazonian flank show temporary loss of biota in the Holocene: The Holocene, v. 22, no. 11, p. 1227-1241.

Goodwin, I. D., Browning, S., Lorrey, A. M., Mayewski, P. A., Phipps, S. J., Bertler, N. A. N., Edwards, R. P., Cohen, T. J., van Ommen, T., Curran, M., Barr, C., and Stager, J. C., 2014, A reconstruction of extratropical Indo-Pacific sea-level pressure patterns during the Medieval Climate Anomaly: Climate Dynamics, v. 43, no. 5, p. 1197-1219.

Graham, N. E., Ammann, C. M., Fleitmann, D., Cobb, K. M., and Luterbacher, J., 2011, Support for global climate reorganization during the “Medieval Climate Anomaly”: Climate Dynamics, v. 37, no. 5, p. 1217-1245.

Gu, F., Chiessi, C. M., Zonneveld, K. A. F., and Behling, H., 2018, Late Quaternary environmental dynamics inferred from marine sediment core GeoB6211-2 off southern Brazil: Palaeogeography, Palaeoclimatology, Palaeoecology, v. 496, p. 48-61.

Guiñez, M., Valdés, J., Sifeddine, A., Boussafir, M., and Dávila, P. M., 2014, Anchovy population and ocean-climatic fluctuations in the Humboldt Current System during the last 700years and their implications: Palaeogeography, Palaeoclimatology, Palaeoecology, v. 415, p. 210-224.

Gusev, A. A., and Martin, I. M., 2012, Possible evidence of the resonant influence of solar forcing on the climate system: Journal of Atmospheric and Solar-Terrestrial Physics, v. 80, no. 0, p. 173-178.

Gutiérrez, D., Bouloubassi, I., Sifeddine, A., Purca, S., Goubanova, K., Graco, M., Field, D., Méjanelle, L., Velazco, F., Lorre, A., Salvatteci, R., Quispe, D., Vargas, G., Dewitte, B., and Ortlieb, L., 2011, Coastal cooling and increased productivity in the main upwelling zone off Peru since the mid-twentieth century: Geophysical Research Letters, v. 38, no. 7.

Hardy, D. R., Vuille, M., and Bradley, R. S., 2003, Variability of snow accumulation and isotopic composition on Nevado Sajama, Bolivia: Journal of Geophysical Research: Atmospheres, v. 108, no. D22.

Hassan, D., Iqbal, A., Ahmad Hassan, S., Abbas, S., and Ansari, M. R. K., 2016, Sunspots and ENSO relationship using Markov method: Journal of Atmospheric and Solar-Terrestrial Physics, v. 137, no. Supplement C, p. 53-57.

Haug, G. H., Günther, D., Peterson, L. C., Sigman, D. M., Hughen, K. A., and Aeschlimann, B., 2003, Climate and the Collapse of Maya Civilization: Science, v. 299, no. 5613, p. 1731-1735.

Haug, G. H., Hughen, K. A., Sigman, D. M., Peterson, L. C., and Röhl, U., 2001, Southward Migration of the Intertropical Convergence Zone Through the Holocene: Science, v. 293, no. 5533, p. 1304-1308.

Henke, L. M. K., Lambert, F. H., and Charman, D. J., 2017, Was the Little Ice Age more or less El Niño-like than the Medieval Climate Anomaly? Evidence from hydrological and temperature proxy data: Clim. Past, v. 13, no. 3, p. 267-301.

Heredia, T., and Elias, A. G., 2013, A study on possible solar and geomagnetic effects on the precipitation over northwestern Argentina: Advances in Space Research, v. 51, no. 10, p. 1883-1892.

Hernández, A., Giralt, S., Bao, R., Sáez, A., Leng, M. J., and Barker, P. A., 2010, ENSO and solar activity signals from oxygen isotopes in diatom silica during late glacial-Holocene transition in Central Andes (18°S): Journal of Paleolimnology, v. 44, no. 2, p. 413-429.

Hessl, A., Allen, K. J., Vance, T., Abram, N. J., and Saunders, K. M., 2017, Reconstructions of the southern annular mode (SAM) during the last millennium: Progress in Physical Geography, v. 0, no. 0, p. 0309133317743165.

Huang, J., Wang, S., Gong, D., Zhou, T., Wen, X., Zhang, Z., and Zhu, J., 2010, Atmospheric oscillations over the last millennium: Chinese Science Bulletin, v. 55, no. 22, p. 2469-2472.

IPCC, 2007, Climate Change 2007: Synthesis Report: http://www.ipcc.ch/publications_and_data/publications_and_data_reports.shtml.

Iriondo, M. n., 1999, Climatic changes in the South American plains: Records of a continent-scale oscillation: Quaternary International, v. 57-58, p. 93-112.

Jalabert, R. B. U., 2002, Desarrollo de una cronología de anchos de anillos para alerce (Fitzroya cupressoides) y reconstrucción de la historia de incendios en el área de Abtao, Parque Nacional Chiloé, X Región [Ingeniero Forestal degree: Pontificia Universidad Católica de Chile.

Jantz, N., and Behling, H., 2012, A Holocene environmental record reflecting vegetation, climate, and fire variability at the Páramo of Quimsacocha, southwestern Ecuadorian Andes: Vegetation History and Archaeobotany, v. 21, no. 3, p. 169-185.

Jenny, B., Valero-Garcés, B. L., Urrutia, R., Kelts, K., Veit, H., Appleby, P. G., and Geyh, M., 2002, Moisture changes and fluctuations of the Westerlies in Mediterranean Central Chile during the last 2000 years: The Laguna Aculeo record (33°50′S): Quaternary International, v. 87, no. 1, p. 3-18.

Jomelli, V., Favier, V., Rabatel, A., Brunstein, D., Hoffmann, G., and Francou, B., 2009, Fluctuations of glaciers in the tropical Andes over the last millennium and palaeoclimatic implications: A review: Palaeogeography, Palaeoclimatology, Palaeoecology, v. 281, no. 3, p. 269-282.

Kämpf, J., and Chapman, P., 2016, Upwelling Systems of the World, Springer International Publishing.

Kaplan, M. R., Schaefer, J. M., Strelin, J. A., Denton, G. H., Anderson, R. F., Vandergoes, M. J., Finkel, R. C., Schwartz, R., Travis, S. G., Garcia, J. L., Martini, M. A., and Nielsen, S. H. H., 2016, Patagonian and southern South Atlantic view of Holocene climate: Quaternary Science Reviews, v. 141, p. 112-125.

Kastner, S., Enters, D., Ohlendorf, C., Haberzettl, T., Kuhn, G., Lücke, A., Mayr, C., Reyss, J.-L., Wastegård, S., and Zolitschka, B., 2010, Reconstructing 2000 years of hydrological variation derived from laminated proglacial sediments of Lago del Desierto at the eastern margin of the South Patagonian Ice Field, Argentina: Global and Planetary Change, v. 72, no. 3, p. 201-214.

Kayano, M. T., and Capistrano, V. B., 2014, How the Atlantic multidecadal oscillation (AMO) modifies the ENSO influence on the South American rainfall: International Journal of Climatology, v. 34, no. 1, p. 162-178.

Kellerhals, T., Brütsch, S., Sigl, M., Knüsel, S., Gäggeler, H. W., and Schwikowski, M., 2010, Ammonium concentration in ice cores: A new proxy for regional temperature reconstruction?: Journal of Geophysical Research: Atmospheres, v. 115, no. D16, p. n/a-n/a.

Kilian, R., Baeza, O., Breuer, S., Ríos, F., Arz, H., Lamy, F., Wirtz, J., Baque, D., Korf, P., Kremer, K., Ríos, C., Mutschke, E., Simon, M., De Pol-Holz, R., Arevalo, M., Wörner, G., Schneider, C., and Casassa, G., 2013, Late Glacial and Holocene Paleogeographical and Paleoecological Evolution of the Seno Skyring and Otway Fjord Systems in the Magellan Region: Anales del Instituto de la Patagonia, v. 41, p. 5-26.

Kilian, R., Schneider, C., Koch, J., Fesq-Martin, M., Biester, H., Casassa, G., Arévalo, M., Wendt, G., Baeza, O., and Behrmann, J., 2007, Palaeoecological constraints on late Glacial and Holocene ice retreat in the Southern Andes (53°S): Global and Planetary Change, v. 59, no. 1, p. 49-66.

Koch, J., and Kilian, R., 2005, 'Little Ice Age' glacier fluctuations, Gran Campo Nevado, southernmost Chile: The Holocene, v. 15, no. 1, p. 20-28.

Köppen, W., 1918, Klassification der Klimate nach Temperatur, Niederschlag and Jahreslauf: Petermanns Geographische Mitteilungen, p. 64. pp.

Kuroda, Y., and Kodera, K., 2005, Solar cycle modulation of the Southern Annular Mode: Geophysical Research Letters, v. 32, no. 13, p. n/a-n/a.

Lamb, H. H., 1965, The early medieval warm epoch and its sequel: Palaeogeogr. Palaeoclim. Palaeoecol., v. 1, p. 13-37.

Lamy, F., Rühlemann, C., Hebbeln, D., and Wefer, G., 2002, High- and low-latitude climate control on the position of the southern Peru-Chile Current during the Holocene: Paleoceanography, v. 17, no. 2, p. 16-11-16-10.

Lea, D. W., Pak, D. K., Peterson, L. C., and Hughen, K. A., 2003, Synchroneity of Tropical and High-Latitude Atlantic Temperatures over the Last Glacial Termination: Science, v. 301, no. 5638, p. 1361-1364.

Lean, J. L., 2018, Estimating Solar Irradiance Since 850 CE: Earth and Space Science.

Lechleitner, F. A., Breitenbach, S. F. M., Rehfeld, K., Ridley, H. E., Asmerom, Y., Prufer, K. M., Marwan, N., Goswami, B., Kennett, D. J., Aquino, V. V., Polyak, V., Haug, G. H., Eglinton, T. I., and Baldini, J. U. L., 2017, Tropical rainfall over the last two millennia: evidence for a low-latitude hydrologic seesaw: Scientific Reports, v. 7, p. 45809.

Lessa, D. V., Venancio, I. M., Santos, T. P. d., Belem, A. L., Turcq, B. J., Sifeddine, A., and Albuquerque, A. L. S., 2016, Holocene oscillations of Southwest Atlantic shelf circulation based on planktonic foraminifera from an upwelling system (off Cabo Frio, Southeastern Brazil): The Holocene, v. 26, no. 8, p. 1175-1187.

Lessa, D. V. d. O., Ramos, R. P., Barbosa, C. F., da Silva, A. R., Belem, A., Turcq, B., and Albuquerque, A. L., 2014, Planktonic foraminifera in the sediment of a western boundary upwelling system off Cabo Frio, Brazil: Marine Micropaleontology, v. 106, p. 55-68.

Letelier, J., Pizarro, O., and Nuñez, S., 2009, Seasonal variability of coastal upwelling and the upwelling front off central Chile: Journal of Geophysical Research: Oceans, v. 114, no. C12.

Li, D., and Xiao, Z., 2018, Can solar cycle modulate the ENSO effect on the Pacific/North American pattern?: Journal of Atmospheric and Solar-Terrestrial Physics, v. 167, p. 30-38.

Liau, J.-R., and Chao, B. F., 2017, Variation of Antarctic circumpolar current and its intensification in relation to the southern annular mode detected in the time-variable gravity signals by GRACE satellite: Earth, Planets and Space, v. 69, no. 1, p. 93.

Liu, Y., Xie, L., Morrison, J. M., Kamykowski, D., and Sweet, W. V., 2014, Ocean Circulation and Water Mass Characteristics around the Galápagos Archipelago Simulated by a Multiscale Nested Ocean Circulation Model: International Journal of Oceanography, v. 2014, p. 16.

Lüning, S., Gałka, M., Danladi, I. B., Adagunodo, T. A., and Vahrenholt, F., 2018, Hydroclimate in Africa during the Medieval Climate Anomaly: Palaeogeography, Palaeoclimatology, Palaeoecology, v. 495, p. 309-322.

Lüning, S., Gałka, M., and Vahrenholt, F., 2017, Warming and Cooling: The Medieval Climate Anomaly in Africa and Arabia: Paleoceanography, v. 32, no. 11, p. 1219-1235.

MacDonald, G. M., and Case, R. A., 2005, Variations in the Pacific Decadal Oscillation over the past millennium: Geophysical Research Letters, v. 32, p. 1-4.

Mahiques, M. M. d., Bícego, M. C., Silveira, I. C. A., Sousa, S. H. M., Lourenço, R. A., and Fukumoto, M. M., 2005, Modern sedimentation in the Cabo Frio upwelling system, Southeastern Brazilian shelf: Anais da Academia Brasileira de Ciências, v. 77, p. 535-548.

Mann, M. E., 2002, Medieval Climatic Optimum, *in* MacCracken, M. C., and Perry, J. S., eds., Encyclopedia of Global Environmental Change: Chichester, John Wiley & Sons, Ltd, p. 514-516.

Mann, M. E., Zhang, Z., Hughes, M. K., Bradley, R. S., Miller, S. K., Rutherford, S., and Ni, F., 2008, Proxy-based reconstructions of hemispheric and global surface temperature variations over the past two millennia: PNAS, v. 105, no. 36, p. 13252-13257.

Mann, M. E., Zhang, Z., Rutherford, S., Bradley, R. S., Hughes, M. K., Shindell, D., Ammann, C., Faluvegi, G., and Ni, F., 2009, Global Signatures and Dynamical Origins of the

Little Ice Age and Medieval Climate Anomaly: Science, v. 326, no. 5957, p. 1256-1260.

Marcott, S. A., Shakun, J. D., Clark, P. U., and Mix, A. C., 2013, A Reconstruction of Regional and Global Temperature for the Past 11,300 Years: Science, v. 339, no. 6124, p. 1198-1201.

Martel-Cea, A., Maldonado, A., Grosjean, M., Alvial, I., de Jong, R., Fritz, S. C., and von Gunten, L., 2016, Late Holocene environmental changes as recorded in the sediments of high Andean Laguna Chepical, Central Chile (32°S; 3050ma.s.l.): Palaeogeography, Palaeoclimatology, Palaeoecology, v. 461, p. 44-54.

Martin, L., Fournier, M., Mourguiart, P., Sifeddine, A., Turcq, B., Flexor, J.-M., and Absy, M. L., 1993, Southern Oscillation Signal in South American Palaeoclimatic Data of the Last 7000 Years: Quaternary Research, v. 39, no. 3, p. 338-346.

Martínez-Ortiz, J., Aires-da-Silva, A. M., Lennert-Cody, C. E., and Maunder, M. N., 2015, The Ecuadorian Artisanal Fishery for Large Pelagics: Species Composition and Spatio-Temporal Dynamics: PLOS ONE, v. 10, no. 8, p. e0135136.

Martínez, J. I., Obrochta, S., Yokoyama, Y., and Battarbee, R. W., 2015, Atlantic Multidecadal Oscillation (AMO) forcing on the late Holocene Cauca paleolake dynamics, northern Andes of Colombia: Clim. Past Discuss., v. 2015, p. 2649-2664.

Masiokas, M. H., Luckman, B. H., Villalba, R., Ripalta, A., and Rabassa, J., 2010, Little Ice Age fluctuations of Glaciar Río Manso in the North Patagonian Andes of Argentina: Quaternary Research, v. 73, no. 1, p. 96-106.

Masiokas, M. H., Rivera, A., Espizua, L. E., Villalba, R., Delgado, S., and Aravena, J. C., 2009, Glacier fluctuations in extratropical South America during the past 1000years: Palaeogeography, Palaeoclimatology, Palaeoecology, v. 281, no. 3, p. 242-268.

Matthews-Bird, F., Brooks, S. J., Holden, P. B., Montoya, E., and Gosling, W. D., 2016, Inferring late-Holocene climate in the Ecuadorian Andes using a chironomid-based temperature inference model: Clim. Past, v. 12, no. 5, p. 1263-1280.

Mauas, P. J. D., Buccino, A. P., and Flamenco, E., 2011, Long-term solar activity influences on South American rivers: Journal of Atmospheric and Solar-Terrestrial Physics, v. 73, no. 2-3, p. 377-382.

McGregor, H. V., Evans, M. N., Goosse, H., Leduc, G., Martrat, B., Addison, J. A., Mortyn, P. G., Oppo, D. W., Seidenkrantz, M.-S., Sicre, M.-A., Phipps, S. J., Selvaraj, K., Thirumalai, K., Filipsson, H. L., and Ersek, V., 2015, Robust global ocean cooling trend for the pre-industrial Common Era: Nature Geoscience, v. 8, p. 671.

Mehta, V. M., and Lau, K. M., 1997, Influence of solar irradiance on the Indian Monsoon-ENSO relationship at decadal-multidecadal time scales: Geophysical Research Letters, v. 24, no. 2, p. 159-162.

Mohtadi, M., Romero, O. E., Kaiser, J., and Hebbeln, D., 2007, Cooling of the southern high latitudes during the Medieval Period and its effect on ENSO: Quaternary Science Reviews, v. 26, no. 7, p. 1055-1066.

Moreira-Turcq, P., Turcq, B., Moreira, L. S., Amorim, M., Cordeiro, R. C., and Guyot, J. L., 2014, A 2700calyr BP extreme flood event revealed by sediment accumulation in Amazon floodplains: Palaeogeography, Palaeoclimatology, Palaeoecology, v. 415, p. 175-182.

Moscol Olivera, M. C., and Hooghiemstra, H., 2010, Three millennia upper forest line changes in northern Ecuador: Pollen records and altitudinal vegetation distributions: Review of Palaeobotany and Palynology, v. 163, no. 1, p. 113-126.

Moy, C. M., Moreno, P. I., Dunbar, R. B., Kaplan, M. R., Francois, J.-P., Villalba, R., and Haberzettl, T., 2009, Climate Change in Southern South America During the Last Two Millennia, *in* Vimeux, F., Sylvestre, F., and Khodri, M., eds., Past Climate Variability in South America and Surrounding Regions: From the Last Glacial Maximum to the Holocene: Dordrecht, Springer Netherlands, p. 353-393.

Moy, C. M., Seltzer, G. O., Rodbell, D. T., and Anderson, D. M., 2002, Variability of El Niño/Southern Oscillation activity at millennial timescales during the Holocene epoch: Nature, v. 420, p. 162.

Mühlinghaus, C., Scholz, D., and Mangini, A., 2008, Temperature and precipitation records from stalagmites grown under disequilibrium conditions: A first approach: PAGES news, v. 16, no. 3, p. 19-20.

Muñoz, P., Gorin, G., Parra, N., Velásquez, C., Lemus, D., Monsalve-M, C., and Jojoa, M., 2017, Holocene climatic variations in the Western Cordillera of Colombia: A multiproxy high-resolution record unravels the dual influence of ENSO and ITCZ: Quaternary Science Reviews, v. 155, p. 159-178.

Muscheler, R., Adolphi, F., Herbst, K., and Nilsson, A., 2016, The Revised Sunspot Record in Comparison to Cosmogenic Radionuclide-Based Solar Activity Reconstructions: Solar Physics, v. 291, no. 9, p. 3025-3043.

Narayan, N., Paul, A., Mulitza, S., and Schulz, M., 2010, Trends in coastal upwelling intensity during the late 20th century: Ocean Sci., v. 6, no. 3, p. 815-823.

Neukom, R., Gergis, J., Karoly, D. J., Wanner, H., Curran, M., Elbert, J., Gonzalez-Rouco, F., Linsley, B. K., Moy, A. D., Mundo, I., Raible, C. C., Steig, E. J., van Ommen, T., Vance, T., Villalba, R., Zinke, J., and Frank, D., 2014, Inter-hemispheric temperature variability over the past millennium: Nature Clim. Change, v. 4, no. 5, p. 362-367.

Neukom, R., Luterbacher, J., Villalba, R., Küttel, M., Frank, D., Jones, P. D., Grosjean, M., Wanner, H., Aravena, J.-C., Black, D. E., Christie, D. A., D’Arrigo, R., Lara, A., Morales, M., Soliz-Gamboa, C., Srur, A., Urrutia, R., and von Gunten, L., 2011, Multiproxy summer and winter surface air temperature field reconstructions for southern South America covering the past centuries: Climate Dynamics, v. 37, no. 1-2, p. 35-51.

Nordemann, D. J. R., Rigozo, N. R., and de Faria, H. H., 2005, Solar activity and El-Niño signals observed in Brazil and Chile tree ring records: Advances in Space Research, v. 35, no. 5, p. 891-896.

Novello, V. F., Cruz, F. W., Karmann, I., Burns, S. J., Stríkis, N. M., Vuille, M., Cheng, H., Lawrence Edwards, R., Santos, R. V., Frigo, E., and Barreto, E. A. S., 2012, Multidecadal climate variability in Brazil's Nordeste during the last 3000 years based on speleothem isotope records: Geophysical Research Letters, v. 39, no. 23.

Novello, V. F., Cruz, F. W., Moquet, J. S., Vuille, M., Paula, M. S., Nunes, D., Edwards, R. L., Cheng, H., Karmann, I., Utida, G., Stríkis, N. M., and Campos, J. L. P. S., 2018, Two Millennia of South Atlantic Convergence Zone Variability Reconstructed From Isotopic Proxies: Geophysical Research Letters, v. 45, no. 10, p. 5045-5051.

Novello, V. F., Cruz, F. W., Vuille, M., Stríkis, N. M., Edwards, R. L., Cheng, H., Emerick, S., de Paula, M. S., Li, X., Barreto, E. d. S., Karmann, I., and Santos, R. V., 2017, A high-resolution history of the South American Monsoon from Last Glacial Maximum to the Holocene: Scientific Reports, v. 7, p. 44267.

Novello, V. F., Vuille, M., Cruz, F. W., Stríkis, N. M., de Paula, M. S., Edwards, R. L., Cheng, H., Karmann, I., Jaqueto, P. F., Trindade, R. I. F., Hartmann, G. A., and Moquet, J. S., 2016, Centennial-scale solar forcing of the South American Monsoon System recorded in stalagmites: Scientific Reports, v. 6, p. 24762.

Nürnberg, D., Böschen, T., Doering, K., Mollier-Vogel, E., Raddatz, J., and Schneider, R., 2015, Sea surface and subsurface circulation dynamics off equatorial Peru during the last ~17 kyr: Paleoceanography, v. 30, no. 7, p. 984-999.

Nuzhdina, M. A., 2002, Connection between ENSO phenomena and solar and geomagnetic activity: Natural Hazards and Earth System Sciences, v. 2, p. 83-89.

Obelic, B., Alvarez, A., Argullós, J., and Piana, E., 1998, Determination of water paleotemperature in the Beagle Channel (Argentina) during the last 6000 yr through stable isotope composition of Mytilusedulis shells: Quaternary of South America and Antarctic Peninsula, v. 11, p. 47-71.

Oyarzún, D., and Brierley, C. M., 2018, The future of coastal upwelling in the Humboldt current from model projections: Climate Dynamics.

PAGES 2k Consortium, 2013, Continental-scale temperature variability during the past two millennia: Nature Geosci, v. 6, no. 5, p. 339-346.

-, 2017, A global multiproxy database for temperature reconstructions of the Common Era: Scientific Data, https://www.ncdc.noaa.gov/paleo-search/study/21171, v. 4.

Palma, E. D., and Matano, R. P., 2009, Disentangling the upwelling mechanisms of the South Brazil Bight: Continental Shelf Research, v. 29, no. 11, p. 1525-1534.

Palóczy, A., da Silveira, I. C. A., Castro, B. M., and Calado, L., 2014, Coastal upwelling off Cape São Tomé (22°S, Brazil): The supporting role of deep ocean processes: Continental Shelf Research, v. 89, p. 38-50.

Perone, A., Lombardi, F., Marchetti, M., Tognetti, R., and Lasserre, B., 2016, Evidence of solar activity and El Niño signals in tree rings of Araucaria araucana and A. angustifolia in South America: Global and Planetary Change, v. 145, p. 1-10.

Peterson, L. C., and Haug, G. H., 2006, Variability in the mean latitude of the Atlantic Intertropical Convergence Zone as recorded by riverine input of sediments to the Cariaco Basin (Venezuela): Palaeogeography, Palaeoclimatology, Palaeoecology, v. 234, no. 1, p. 97-113.

Piola, A. R., and Matano, R. P., 2017, Ocean Currents: Atlantic Western Boundary—Brazil Current/Falkland (Malvinas), Reference Module in Earth Systems and Environmental Sciences, Elsevier.

Pivel, M. A. G., Santarosa, A. C. A., Toledo, F. A. L., and Costa, K. B., 2013, The Holocene onset in the southwestern South Atlantic: Palaeogeography, Palaeoclimatology, Palaeoecology, v. 374, p. 164-172.

Polissar, P. J., Abbott, M. B., Wolfe, A. P., Bezada, M., Rull, V., and Bradley, R. S., 2006, Solar modulation of Little Ice Age climate in the tropical Andes: Proceedings of the National Academy of Sciences, v. 103, no. 24, p. 8937-8942.

Ponce, J. F., Borromei, A. M., Menounos, B., and Rabassa, J., 2017, Late-Holocene and Little Ice Age palaeoenvironmental change inferred from pollen analysis, Isla de los Estados, Argentina: Quaternary International, v. 442, p. 26-34.

Ponce, J. F., Borromei, A. M., Rabassa, J. O., and Martinez, O., 2011, Late Quaternary palaeoenvironmental change in western Staaten Island (54.5° S, 64° W), Fuegian Archipelago: Quaternary International, v. 233, no. 2, p. 89-100.

Prestes, A., R.Rigozo, N., Nordemann, D. J. R., Wrasse, C. M., Souza Echer, M. P., Echer, E., da Rosa, M. B., and Rampelotto, P. H., 2011, Sun–earth relationship inferred by tree growth rings in conifers from Severiano De Almeida, Southern Brazil: Journal of Atmospheric and Solar-Terrestrial Physics, v. 73, p. 1587-1593.

Rabatel, A., Francou, B., Soruco, A., Gomez, J., Cáceres, B., Ceballos, J. L., Basantes, R., Vuille, M., Sicart, J. E., Huggel, C., Scheel, M., Lejeune, Y., Arnaud, Y., Collet, M., Condom, T., Consoli, G., Favier, V., Jomelli, V., Galarraga, R., Ginot, P., Maisincho, L., Mendoza, J., Ménégoz, M., Ramirez, E., Ribstein, P., Suarez, W., Villacis, M., and Wagnon, P., 2013, Current state of glaciers in the tropical Andes: a multi-century perspective on glacier evolution and climate change: The Cryosphere, v. 7, no. 1, p. 81-102.

Rabatel, A., Jomelli, V., Naveau, P., Francou, B., and Grancher, D., 2005, Dating of Little Ice Age glacier fluctuations in the tropical Andes: Charquini glaciers, Bolivia, 16°S: Comptes Rendus Geoscience, v. 337, no. 15, p. 1311-1322.

Ramirez, E., Hoffmann, G., Taupin, J. D., Francou, B., Ribstein, P., Caillon, N., Ferron, F. A., Landais, A., Petit, J. R., Pouyaud, B., Schotterer, U., Simoes, J. C., and Stievenard, M., 2003, A new Andean deep ice core from Nevado Illimani (6350 m), Bolivia: Earth and Planetary Science Letters, v. 212, no. 3, p. 337-350.

Rein, B., Lückge, A., and Sirocko, F., 2004, A major Holocene ENSO anomaly during the Medieval period: Geophysical Research Letters, v. 31, no. 17.

Reuter, J., Stott, L., Khider, D., Sinha, A., Cheng, H., and Edwards, R. L., 2009, A new perspective on the hydroclimate variability in northern South America during the Little Ice Age: Geophysical Research Letters, v. 36, no. 21.

Rigozo, N. R., da Silva, H. E., Nordemann, D. J. R., Echer, E., de Souza Echer, M. P., and Prestes, A., 2008a, The Medieval and Modern Maximum solar activity imprints in tree ring data from Chile and stable isotope records from Antarctica and Peru: Journal of Atmospheric and Solar-Terrestrial Physics, v. 70, no. 7, p. 1012-1024.

Rigozo, N. R., Jean Roger Nordemann, D., Echer, E., Evangelista da Silva, H., Pereira de Souza Echer, M., and Prestes, A., 2007, Solar and climate imprint differences in tree ring width from Brazil and Chile: Journal of Atmospheric and Solar-Terrestrial Physics, v. 69, no. 4, p. 449-458.

Rigozo, N. R., Prestes, A., Nordemann, D. J. R., da Silva, H. E., Souza Echer, M. P., and Echer, E., 2008b, Solar maximum epoch imprints in tree-ring width from Passo Fundo, Brazil (1741–2004): Journal of Atmospheric and Solar-Terrestrial Physics, v. 70, no. 7, p. 1025-1033.

Rivera, A., Koppes, M., Bravo, C., and Aravena, J. C., 2012, Little ice age advance and retreat of Glaciar Jorge Montt, Chilean Patagonia, recorded in maps, air photographs and dendrochronology: Clim. Past, v. 8, p. 403-414.

Rosso, F. V., Boiaski, N. T., Ferraz, S. E. T., Dewes, C. F., and Tatsch, J. D., 2015, Trends and Decadal Variability in Air Temperature over Southern Brazil: American Journal of Environmental Engineering, v. 5, no. 1A, p. 85-95.

Roy, I., and Haigh, J. D., 2011, The influence of solar variability and the quasi-biennial oscillation on lower atmospheric temperatures and sea level pressure: Atmos. Chem. Phys., v. 11, no. 22, p. 11679-11687.

Rueda-Roa, D. T., and Muller-Karger, F. E., 2013, The southern Caribbean upwelling system: Sea surface temperature, wind forcing and chlorophyll concentration patterns: Deep Sea Research Part I: Oceanographic Research Papers, v. 78, p. 102-114.

Rull, V., Salgado-Labouriau, M. L., Schubert, C., and Valastro, S., 1987, Late holocene temperature depression in the Venezuelan andes: Palynological evidence: Palaeogeography, Palaeoclimatology, Palaeoecology, v. 60, p. 109-121.

Rull, V., and Schubert, C., 1989, The Little Ice Age in the tropical Venezuelan Andes: Acta científica venezolana, v. 40, p. 71-73.

Rustic, G. T., Koutavas, A., Marchitto, T. M., and Linsley, B. K., 2015, Dynamical excitation of the tropical Pacific Ocean and ENSO variability by Little Ice Age cooling: Science, v. 350, no. 6267, p. 1537-1541.

Salas, I., Herrera, C., Luque, J. A., Delgado, J., Urrutia, J., and Jordan, T., 2016, Recent climatic events controlling the hydrological and the aquifer dynamics at arid areas: The case of Huasco River watershed, northern Chile: Science of The Total Environment, v. 571, no. Supplement C, p. 178-194.

Salvador, M. d. A., and de Brito, J. I. B., 2017, Trend of annual temperature and frequency of extreme events in the MATOPIBA region of Brazil: Theoretical and Applied Climatology.

Salvatteci, R., Gutiérrez, D., Field, D., Sifeddine, A., Ortlieb, L., Bouloubassi, I., Boussafir, M., Boucher, H., and Cetin, F., 2014, The response of the Peruvian Upwelling Ecosystem to centennial-scale global change during the last two millennia: Clim. Past, v. 10, no. 2, p. 715-731.

Salvatteci, R., Gutierrez, D., Sifeddine, A., Ortlieb, L., Druffel, E., Boussafir, M., and Schneider, R., 2016, Centennial to millennial-scale changes in oxygenation and productivity in the Eastern Tropical South Pacific during the last 25,000 years: Quaternary Science Reviews, v. 131, p. 102-117.

Salzmann, N., Huggel, C., Rohrer, M., Silverio, W., Mark, B. G., Burns, P., and Portocarrero, C., 2013, Glacier changes and climate trends derived from multiple sources in the data scarce Cordillera Vilcanota region, southern Peruvian Andes: The Cryosphere, v. 7, no. 1, p. 103-118.

Santos, T. P., Franco, D. R., Barbosa, C. F., Belem, A. L., Dokken, T., and Albuquerque, A. L. S., 2013, Millennial- to centennial-scale changes in sea surface temperature in the tropical South Atlantic throughout the Holocene: Palaeogeography, Palaeoclimatology, Palaeoecology, v. 392, p. 1-8.

Saurral, R. I., Doblas-Reyes, F. J., and García-Serrano, J., 2018, Observed modes of sea surface temperature variability in the South Pacific region: Climate Dynamics, v. 50, no. 3, p. 1129-1143.

Schauwecker, S., Rohrer, M., Acuña, D., Cochachin, A., Dávila, L., Frey, H., Giráldez, C., Gómez, J., Huggel, C., Jacques-Coper, M., Loarte, E., Salzmann, N., and Vuille, M., 2014, Climate trends and glacier retreat in the Cordillera Blanca, Peru, revisited: Global and Planetary Change, v. 119, p. 85-97.

Schellekens, J., Horák-Terra, I., Buurman, P., Silva, A. C., and Vidal-Torrado, P., 2014, Holocene vegetation and fire dynamics in central-eastern Brazil: Molecular records from the Pau de Fruta peatland: Organic Geochemistry, v. 77, p. 32-42.

Schneider, W., Donoso, D., Garcés-Vargas, J., and Escribano, R., 2017, Water-column cooling and sea surface salinity increase in the upwelling region off central-south Chile driven by a poleward displacement of the South Pacific High: Progress in Oceanography, v. 151, p. 38-48.

Seillès, B., Goñi, M. F. S., Ledru, M.-P., Urrego, D. H., Martinez, P., Hanquiez, V., and Schneider, R., 2016, Holocene land–sea climatic links on the equatorial Pacific coast (Bay of Guayaquil, Ecuador): The Holocene, v. 26, no. 4, p. 567-577.

Sepúlveda, J., Pantoja, S., Hughen, K. A., Bertrand, S., Figueroa, D., León, T., Drenzek, N. J., and Lange, C., 2009, Late Holocene sea-surface temperature and precipitation variability in northern Patagonia, Chile (Jacaf Fjord, 44°S): Quaternary Research, v. 72, no. 3, p. 400-409.

Siani, G., Michel, E., De Pol-Holz, R., DeVries, T., Lamy, F., Carel, M., Isguder, G., Dewilde, F., and Lourantou, A., 2013, Carbon isotope records reveal precise timing of enhanced Southern Ocean upwelling during the last deglaciation: Nature Communications, v. 4, p. 2758.

Sigl, M., Winstrup, M., McConnell, J. R., Welten, K. C., Plunkett, G., Ludlow, F., Buntgen, U., Caffee, M., Chellman, N., Dahl-Jensen, D., Fischer, H., Kipfstuhl, S., Kostick, C., Maselli, O. J., Mekhaldi, F., Mulvaney, R., Muscheler, R., Pasteris, D. R., Pilcher, J.

R., Salzer, M., Schupbach, S., Steffensen, J. P., Vinther, B. M., and Woodruff, T. E., 2015, Timing and climate forcing of volcanic eruptions for the past 2,500 years: Nature, v. 523, no. 7562, p. 543-549.

Soares, D. d. B., Lee, H., Loikith, P. C., Barkhordarian, A., and Mechoso, C. R., 2017, Can significant trends be detected in surface air temperature and precipitation over South America in recent decades?: International Journal of Climatology, v. 37, no. 3, p. 1483-1493.

Solomina, O. N., Bradley, R. S., Jomelli, V., Geirsdottir, A., Kaufman, D. S., Koch, J., McKay, N. P., Masiokas, M., Miller, G., Nesje, A., Nicolussi, K., Owen, L. A., Putnam, A. E., Wanner, H., Wiles, G., and Yang, B., 2016, Glacier fluctuations during the past 2000 years: Quaternary Science Reviews, v. 149, p. 61-90.

Souto, D. D., de Oliveira Lessa, D. V., Albuquerque, A. L. S., Sifeddine, A., Turcq, B. J., and Barbosa, C. F., 2011, Marine sediments from southeastern Brazilian continental shelf: A 1200year record of upwelling productivity: Palaeogeography, Palaeoclimatology, Palaeoecology, v. 299, no. 1, p. 49-55.

Stansell, N. D., Abbott, M. B., Polissar, P. J., Wolfe, A. P., Bezada, M., and Rull, V., 2005, Late Quaternary deglacial history of the Mérida Andes, Venezuela: Journal of Quaternary Science, v. 20, no. 7-8, p. 801-812.

Stansell, N. D., Polissar, P. J., Abbott, M. B., Bezada, M., Steinman, B. A., and Braun, C., 2014, Proglacial lake sediment records reveal Holocene climate changes in the Venezuelan Andes: Quaternary Science Reviews, v. 89, p. 44-55.

Stansell, N. D., Rodbell, D. T., Abbott, M. B., and Mark, B. G., 2013, Proglacial lake sediment records of Holocene climate change in the western Cordillera of Peru: Quaternary Science Reviews, v. 70, p. 1-14.

Steinhilber, F., Abreu, J. A., Beer, J., Brunner, I., Christl, M., Fischer, H., Heikkilä, U., Kubik, P. W., Mann, M., McCracken, K. G., Miller, H., Miyahara, H., Oerter, H., and Wilhelms, F., 2012, 9,400 years of cosmic radiation and solar activity from ice cores and tree rings: Proceedings of the National Academy of Sciences, v. 109, no. 16, p. 5967-5971.

Sterken, M., Sabbe, K., Chepstow-Lusty, A., Frogley, M., Vanhoutte, K., Verleyen, E., Cundy, A., and Vyverman, W., 2006, Hydrological and land-use changes in the Cuzco region (Cordillera Oriental, South East Peru) during the last 1200 years: a diatom-based reconstruction: Archiv für Hydrobiologie, v. 165, no. 3, p. 289-312.

Strelin, J., Casassa, G., Rosqvist, G., and Holmlund, P., 2008, Holocene glaciations in the Ema Glacier valley, Monte Sarmiento Massif, Tierra del Fuego: Palaeogeography, Palaeoclimatology, Palaeoecology, v. 260, no. 3, p. 299-314.

Strelin, J. A., Kaplan, M. R., Vandergoes, M. J., Denton, G. H., and Schaefer, J. M., 2014, Holocene glacier history of the Lago Argentino basin, Southern Patagonian Icefield: Quaternary Science Reviews, v. 101, p. 124-145.

Stríkis, N. M., Cruz, F. W., Cheng, H., Karmann, I., Edwards, R. L., Vuille, M., Wang, X., de Paula, M. S., Novello, V. F., and Auler, A. S., 2011, Abrupt variations in South American monsoon rainfall during the Holocene based on a speleothem record from central-eastern Brazil: Geology, v. 39, no. 11, p. 1075-1078.

Stroup, J. S., Kelly, M. A., Lowell, T. V., Applegate, P. J., and Howley, J. A., 2014, Late Holocene fluctuations of Qori Kalis outlet glacier, Quelccaya Ice Cap, Peruvian Andes: Geology, v. 42, no. 4, p. 347-350.

Stroup, J. S., Kelly, M. A., Lowell, T. V., Smith, C. A., Beal, S. A., Landis, J. D., and Tapia, P. M., 2015, Late Holocene fluctuations of Quelccaya Ice Cap, Peru, registered by nearby lake sediments: Journal of Quaternary Science, v. 30, no. 8, p. 830-840.

Sturm, C., Hoffmann, G., and Langmann, B., 2007a, Simulation of the Stable Water Isotopes in Precipitation over South America: Comparing Regional to Global Circulation Models: Journal of Climate, v. 20, no. 15, p. 3730-3750.

Sturm, C., Vimeux, F., and Krinner, G., 2007b, Intraseasonal variability in South America recorded in stable water isotopes: Journal of Geophysical Research: Atmospheres, v. 112, no. D20.

Stutz, S., Borel, C. M., Fontana, S. L., and Tonello, M. S., 2012, Holocene changes in trophic states of shallow lakes from the Pampa plain of Argentina: The Holocene, v. 22, no. 11, p. 1263-1270.

Suby, J., Luna, L., Aranda, C., and Flensborg, G., 2017, First approximation to paleodemography through age-at-death profiles in hunter-gatherers from Southern Patagonia during middle-late Holocene: Quaternary International, v. 438, p. 174-188.

Tarazona, J., and Arntz, W., 2001, The Peruvian Coastal Upwelling System, *in* Seeliger, U., and Kjerfve, B., eds., Coastal Marine Ecosystems of Latin America: Berlin, Heidelberg, Springer Berlin Heidelberg, p. 229-244.

Thiel, M., Macaya, E. C., Acuña, E., Arntz, W. E., Bastias, H., Brokordt, K., Camus, P. A., Castilla, J. C., Castro, L. R., Cortés, M., Dumont, C. P., Escribano, R., Fernandez, M., Gajardo, J. A., Gaymer, C. F., Gomez, I., González, A. E., González, H. E., Haye, P. A., Illanes, J.-E., Iriarte, J. L., Lancellotti, D. A., Luna-Jorquera, G., Luxoro, C., Manriquez, P. H., Marín, V., Muñoz, P., Navarrete, S. A., Perez, E., Poulin, E., Sellanes, J., Sepúlveda, H. H., Stotz, W., Tala, F., Thomas, A., Vargas, C. A., Vasquez, J. A., and Vega, J. M., 2007, The Humboldt Current System of northern and central Chile, *in* Gibson, R. N., Atkinson, R. J. A., and Gordon, J. D. M., eds., Oceanography and Marine Biology: An Annual Review, Volume 45, Taylor & Francis, p. 195-344.

Thompson, L. G., 1995, Late Holocene ice core records of climate and environment from the tropical Andes, Peru: Bull. inst. fr. études andines, v. 24, no. 3, p. 619-629.

Thompson, L. G., Mosley-Thompson, E., Dansgaard, W., and Grootes, P. M., 1986, The Little Ice Age as Recorded in the Stratigraphy of the Tropical Quelccaya Ice Cap: Science, v. 234, no. 4774, p. 361-364.

Thompson, L. G., Mosley-Thompson, E., Davis, M. E., Lin, P.-N., Henderson, K., and Mashiotta, T. A., 2003, Tropical Glacier and Ice Core Evidence of Climate Change on Annual to Millennial Time Scales: Climatic Change, v. 59, no. 1, p. 137-155.

Thompson, L. G., Mosley-Thompson, E., Davis, M. E., Lin, P.-N., Henderson, K. A., Cole-Dai, J., Bolzan, J. F., and Liu, K.-b., 1995, Late Glacial Stage and Holocene Tropical Ice Core Records from Huascarán, Peru: Science, v. 269, no. 5220, p. 46-50.

Thompson, L. G., Mosley-Thompson, E., Davis, M. E., Zagorodnov, V. S., Howat, I. M., Mikhalenko, V. N., and Lin, P.-N., 2013, Annually Resolved Ice Core Records of Tropical Climate Variability over the Past ~1800 Years: Science, v. 340, no. 6135, p. 945-950.

Trouet, V., Scourse, J. D., and Raible, C. C., 2012, North Atlantic storminess and Atlantic Meridional Overturning Circulation during the last Millennium: Reconciling contradictory proxy records of NAO variability: Global and Planetary Change, v. 84-85, p. 48-55.

Turney, C. S. M., Jones, R. T., Fogwill, C., Hatton, J., Williams, A. N., Hogg, A., Thomas, Z. A., Palmer, J., Mooney, S., and Reimer, R. W., 2016, A 250-year periodicity in Southern Hemisphere westerly winds over the last 2600 years: Clim. Past, v. 12, no. 2, p. 189-200.

Usoskin, I. G., Gallet, Y., Lopes, F., Kovaltsov, G. A., and Hulot, G., 2016, Solar activity during the Holocene: the Hallstatt cycle and its consequence for grand minima and maxima⋆: A&A, v. 587, p. A150.

Valentin, J. L., 2001, The Cabo Frio Upwelling System, Brazil, *in* Seeliger, U., and Kjerfve, B., eds., Coastal Marine Ecosystems of Latin America: Berlin, Heidelberg, Springer Berlin Heidelberg, p. 97-105.

Vargas, G., Pantoja, S., Rutllant, J. A., Lange, C. B., and Ortlieb, L., 2007, Enhancement of coastal upwelling and interdecadal ENSO-like variability in the Peru-Chile Current since late 19th century: Geophysical Research Letters, v. 34, no. 13.

Varma, V., Prange, M., Lamy, F., Merkel, U., and Schulz, M., 2011, Solar-forced shifts of the Southern Hemisphere Westerlies during the Holocene: Clim. Past, v. 7, p. 339-347.

Varma, V., Prange, M., Spangehl, T., Lamy, F., Cubasch, U., and Schulz, M., 2012, Impact of solar-induced stratospheric ozone decline on Southern Hemisphere westerlies during the Late Maunder Minimum: Geophys. Res. Lett., v. 39, no. 20, p. L20704.

Veettil, B. K., Wang, S., Bremer, U. F., de Souza, S. F., and Simões, J. C., 2017, Recent trends in annual snowline variations in the northern wet outer tropics: case studies from southern Cordillera Blanca, Peru: Theoretical and Applied Climatology, v. 129, no. 1, p. 213-227.

Velásquez-Ruiz, C. A., and Hooghiemstra, H., 2013, Pollen-based 17-kyr forest dynamics and climate change from the Western Cordillera of Colombia; no-analogue associations and temporarily lost biomes: Review of Palaeobotany and Palynology, v. 194, p. 38-49.

Vilanova, I., Schittek, K., Geilenkirchen, M., Schäbitz, F., and Schulz, W., 2015, Last millennial environmental reconstruction based on a multi-proxy record from Laguna Nassau, Western Pampas, Argentina: Neues Jahrbuch für Geologie und Paläontologie - Abhandlungen, v. 277, no. 2, p. 209-224.

Villacís, M., Vimeux, F., and Taupin, J. D., 2008, Analysis of the climate controls on the isotopic composition of precipitation (δ18O) at Nuevo Rocafuerte, 74.5°W, 0.9°S, 250 m, Ecuador: Comptes Rendus Geoscience, v. 340, no. 1, p. 1-9.

Villalba, R., 1994, Tree-Ring and Glacial Evidence for the Medieval Warm Epoch and the Little Ice Age in Southern South America, *in* Hughes, M. K., and Diaz, H. F., eds., The Medieval Warm Period: Dordrecht, Springer Netherlands, p. 183-197.

Villalba, R., Leiva, J. C., Rubulls, S., Suarez, J., and Lenzano, L., 1990, Climate, Tree-Ring, and Glacial Fluctuations in the Rio Frias Valley, Rio Negro, Argentina: Arctic and Alpine Research, v. 22, no. 3, p. 215-232.

Villota, A., Behling, H., and León-Yánez, S., 2017, Three millennia of vegetation and environmental dynamics in the Lagunas de Mojanda region, northern Ecuador, Acta Palaeobotanica, Volume 57, p. 407.

Vimeux, F., Ginot, P., Schwikowski, M., Vuille, M., Hoffmann, G., Thompson, L. G., and Schotterer, U., 2009, Climate variability during the last 1000 years inferred from Andean ice cores: A review of methodology and recent results: Palaeogeography, Palaeoclimatology, Palaeoecology, v. 281, no. 3, p. 229-241.

Vincent, L. A., Peterson, T. C., Barros, V. R., Marino, M. B., Rusticucci, M., Carrasco, G., Ramirez, E., Alves, L. M., Ambrizzi, T., Berlato, M. A., Grimm, A. M., Marengo, J. A., Molion, L., Moncunill, D. F., Rebello, E., Anunciação, Y. M. T., Quintana, J., Santos, J. L., Baez, J., Coronel, G., Garcia, J., Trebejo, I., Bidegain, M., Haylock, M. R., and Karoly, D., 2005, Observed Trends in Indices of Daily Temperature Extremes in South America 1960–2000: Journal of Climate, v. 18, no. 23, p. 5011-5023.

Voigt, I., Chiessi, C. M., Piola, A. R., and Henrich, R., 2016, Holocene changes in Antarctic Intermediate Water flow strength in the Southwest Atlantic: Palaeogeography, Palaeoclimatology, Palaeoecology, v. 463, p. 60-67.

Voigt, I., Chiessi, C. M., Prange, M., Mulitza, S., Groeneveld, J., Varma, V., and Henrich, R., 2015, Holocene shifts of the southern westerlies across the South Atlantic: Paleoceanography, v. 30, no. 2, p. 39-51.

von Gunten, L., D'Andrea, W. J., Bradley, R. S., and Huang, Y., 2012, Proxy-to-proxy calibration: Increasing the temporal resolution of quantitative climate reconstructions: Scientific Reports, v. 2, p. 609.

von Gunten, L., Grosjean, M., Rein, B., Urrutia, R., and Appleby, P., 2009, A quantitative high-resolution summer temperature reconstruction based on sedimentary pigments from Laguna Aculeo, central Chile, back to AD 850: The Holocene, v. 19, no. 6, p. 873-881.

Vuille, M., Burns, S. J., Taylor, B. L., Cruz, F. W., Bird, B. W., Abbott, M. B., Kanner, L. C., Cheng, H., and Novello, V. F., 2012, A review of the South American monsoon history as recorded in stable isotopic proxies over the past two millennia: Climate of the Past, v. 8, p. 1309-1321.

Vuille, M., Carey, M., Huggel, C., Buytaert, W., Rabatel, A., Jacobsen, D., Soruco, A., Villacis, M., Yarleque, C., Elison Timm, O., Condom, T., Salzmann, N., and Sicart, J.-E., 2018, Rapid decline of snow and ice in the tropical Andes – Impacts, uncertainties and challenges ahead: Earth-Science Reviews, v. 176, p. 195-213.

Vuille, M., Franquist, E., Garreaud, R., Casimiro, W. S. L., and Cáceres, B., 2015, Impact of the global warming hiatus on Andean temperature: Journal of Geophysical Research: Atmospheres, v. 120, no. 9, p. 3745-3757.

Vuille, M., and Werner, M., 2005, Stable isotopes in precipitation recording South American summer monsoon and ENSO variability: observations and model results: Climate Dynamics, v. 25, no. 4, p. 401-413.

Wills, R. C., Schneider, T., Wallace, J. M., Battisti, D. S., and Hartmann, D. L., 2018, Disentangling Global Warming, Multidecadal Variability, and El Niño in Pacific Temperatures: Geophysical Research Letters, v. 45, no. 5, p. 2487-2496.

Yan, H., Sun, L., Wang, Y., Huang, W., Qiu, S., and Yang, C., 2011, A record of the Southern Oscillation Index for the past 2,000 years from precipitation proxies: Nature Geoscience, v. 4, p. 611.